Variability in the redox status of plant 2-Cys peroxiredoxins in relation to species and light cycle

Delphine Cerveau, Patricia Henri, Laurence Blanchard, Pascal Rey

Variability in the redox status of plant 2-Cys peroxiredoxins in relation to species and light cycle

Delphine Cerveau[1], Patricia Henri[1], Laurence Blanchard[2] and Pascal Rey[1, *]

[1] Aix Marseille Univ, CEA, CNRS, BIAM, Plant Protective Proteins Team, Saint Paul-Lez-Durance, France F-13108

[2] Aix Marseille Univ, CEA, CNRS, BIAM, Molecular and Environmental Microbiology Team, Saint Paul-Lez-Durance, France F-13108

Mail adresses :

Delphine Cerveau: delphine.cerveau@yahoo.com

Patricia Henri: patricia.henri@cea.fr

Laurence Blanchard: laurence.blanchard@cea.fr

Pascal Rey: pascal.rey@cea.fr

*Corresponding author: Pascal Rey

Plant Protective Proteins Team, Bâtiment 158, BIAM, CEA Cadarache, Saint-Paul-lez-Durance, F-13108, France

Phone: ++33 442254776

E-mail: pascal.rey@cea.fr

Date of submission: April 9, 2019

Number of tables: 0

Number of figures: 8 (seven in black and white and one in color)

Word count; *ca* 6035

Supplementary data: Four figures

Variability in the redox status of plant 2-Cys peroxiredoxins in relation to species and light cycle

Running title

Variability in the redox status of plant 2-Cys peroxiredoxins

Highlight

Based on the variability in the redox forms of plant 2-Cys peroxiredoxins, we propose that their functions in redox homeostasis are differentially modulated as a function of species.

Abstract

Plant 2-Cys peroxiredoxins (2-CysPRXs) are abundant plastidial thiol-peroxidases involved in key signaling processes such as photosynthesis deactivation at night. Their functions rely on the redox status of their two cysteines and on the enzyme quaternary structure, features for which the knowledge remains poor in plant cells. Using *ex vivo* and biochemical approaches, we thoroughly characterized the 2-CysPRX dimer/monomer distribution, hyperoxidation level, and thiol content in Arabidopsis, barley and potato, in relation to light cycle. Our data reveal that the enzyme hyperoxidization level and its distribution in dimer and monomer vary along the light cycle in a species-dependent manner. A differential susceptibility to hyperoxidation was observed for the two Arabidopsis 2-CysPRX isoforms and among the proteins of the three species, and was associated to sequence variation in hyperoxidation resistance motifs. Alkylation experiments indicate that only a minor fraction of the 2-CysPRX pool carries one free thiol in the three species, and that this content does not change during the light period. We conclude that most plastidial 2-CysPRX forms are oxidized and propose that there is a species-dependent variability in their functions since dimer and hyperoxidized forms fulfill distinct roles regarding direct oxidation of partners and signal transmission.

Keywords

Cysteine, peroxiredoxin, plant, plastid, redox status, signaling, thiol content

Introduction

Peroxiredoxins (PRXs), first identified in yeast (Kim *et al.,* 1989), are ubiquitous thiol-peroxidases reducing H_2O_2 and organic peroxides. The substrate reduction results in oxidation of the thiol group in a sulfenic acid form, and the activity is generally regenerated via the oxidation of thioredoxins (TRXs) (Rhee, 2016). PRXs are classified based on the number (one or two) of redox-active cysteines (Cys) and on the catalytic form (monomer or dimer). The most represented, 2-CysPRXs, are active as a dimer and harbor two conserved Cys termed CysP and CysR for peroxidatic and resolving, respectively (Rhee, 2016). The head-to-tail dimers are formed thanks to one or two covalent bounds between the two Cys. Pro-oxidative conditions lead to peroxidase activity inactivation due to CysP hyperoxidation to a sulfinic acid form, which can be reversed by sulfiredoxin (SRX) (Biteau *et al.,* 2003; Jönsson *et al.,* 2008). In yeast exposed to severe oxidative or heat stresses, 2-CysPRX hyperoxidation results in formation of high molecular weight (HMW) multimers and functional switch from peroxidase to chaperone activity (Jang *et al.,* 2004). Signaling roles have been also unveiled for yeast and animal 2-CysPRXs via the control of peroxide concentration or via direct and sensitive thiol oxidation in protein partners (Day *et al*., 2012; Rhee and Woo, 2011; Stöcker *at al.,* 2017).

In plants, four PRX types are present (Dietz, 2011), three being plastidial: 2-CysPRXs, PRXII-E and PRXQ (Baier and Dietz, 1997; Lamkemeyer *et al.,* 2006; Gama *et al.,* 2008). Typical 2-CysPRXs, first characterized in barley (Baier and Dietz, 1996), are the most abundant since they represent *ca* 1% of plastidial proteins (Dietz *et al.,* 2006). Their hyperoxidation is reversed by SRX (Liu *et al.,* 2006; Rey *et al.,* 2007) and several TRX types reduce them *in vitro*: i) NTRC, NADPH-dependent TRX Reductase C, that contains one TRX domain and one NADPH-dependent TRX reductase domain (Moon *et al.,* 2006; Perez-Ruiz *et al.,* 2006; Perez-Ruiz and Cejudo, 2009); ii) a TRX-like protein termed CDSP32 (Chloroplastic Drought-induced Stress Protein of 32 kDa) (Rey *et al.*, 1998; Broin *et al.,* 2002; Rey *et al*., 2005; Cerveau *et al*., 2016*a*) ; iii) a typical TRX termed TRX x (Collin *et al.,* 2003). In the last years, several functions have been uncovered for plant 2-CysPRXs. Pulido *et al.,* (2010) reported that an Arabidopsis mutant with less than 5% protein displays reduced growth and altered redox homeostasis. Based on the high light sensitivity of a fully knocked-out line, these enzymes were proposed to take part in an alternative water-water cycle to protect photosynthetic membranes (Awad *et al*., 2015). Dangoor *et al.,* (2012) reported that oxidization by 2-CysPRX of the Atypical Cysteine Histidine rich TRX, ACHT1, is associated with altered production of peroxides upon moderate light intensity. They

concluded that ACHT1 could sense and transmit a light-related signal regulating photosynthetic activity. Using a genetic approach, Perez-Ruiz *et al.,* (2017) proposed that the 2-CysPRX redox balance controls photosynthetic metabolism. Consistently, Yoshida *et al.,* (2018), Ojeda *et al.,* (2018), and Vaseghi *et al.,* (2018) showed that the oxidation dynamics of several photosynthetic enzymes was delayed in the Arabidopsis mutant lacking 2-CysPRXs during the light-dark transition. Further, Yoshida *et al.,* (2018) showed that these photosynthetic enzymes are oxidized by the atypical TRX-like2, which can reduce 2-CysPRX *in vitro*, and suggested that the TRX-like2/2-CysPRX redox cascade supports photosynthesis deactivation at night.

The multiple 2-CysPRX functions upon environmental constraints, ageing or diseases (Dietz, 2011; Rhee and Woo, 2011; Rhee, 2016; Liebthal *et al.*, 2018) rely on the redox status of the two Cys residues that greatly condition the protein structural and biochemical features. Of note, human 2-CysPRXs exhibit differential properties with regard to hyperoxidation, likely conferring them distinct functions (Haynes *et al.,* 2013; Bolduc *et al.* 2018). Few data are currently available about the redox status of plant 2-CysPRXs and its possible variability. The two recombinant Arabidopsis isoforms share a similar behavior *in vitro* (Kirchsteiger *et* al., 2009; Puerto-Galan *et al.,* 2015). The dimer/monomer distribution likely varies depending on species since low and high monomer abundances were noticed in potato and Arabidopsis, respectively (Broin and Rey, 2003; Baier and Dietz 1999). Here, we performed a thorough analysis of plant 2-CysPRX redox forms in three representative model and cultivated species that have been the subject of most studies on these thiol-peroxidases, two dicotyledons (Arabidopsis, and potato) and one monocotyledon (barley). Our data reveal that only a minor fraction of the 2-CysPRX pool carries one free thiol and that the dimer/monomer distribution and the hyperoxidation level substantially vary as a function of species and light cycle.

Materials and methods

Plant materials and growth conditions

Arabidopsis plants were grown from sowing in soil in standard conditions under an 8-h photoperiod and a photon flux density of 200 µmol photons.m^{-2}.s^{-1}, 22/18°C (day/night) and 55% relative humidity. Plants were alternatively watered with tap water and nutritive solution (Coic and Lesaint, 1971) every two days. The genotypes used were wild-type Col-0, T-DNA homozygous mutants for *SRX* (SALK_015324) (Rey *et al.,* 2007), *NTRC* (SALK_096776, SALK_012208) (Serrato *et al.,* 2004; Lepisto *et al.,* 2009), *2-CysPRXA* (GK_295C05) and *2-CysPRXB* (SALK_017213). These two last lines were crossed to generate one double mutant

deficient in both *2-CysPRX* genes (Cerveau *et al.,* 2016*b*). Potato (*Solanum tuberosum* cv. Désirée) plantlets were propagated *in vitro* for 3 weeks and transferred in soil in a phytotron under a 12-h photoperiod, 250 µmol photons.m^{-2}.s^{-1} and 24/19°C (day/night). WT and five lines modified for *CDSP32* expression either co-suppressed or over-expressing WT or active-site mutated forms were used (Broin *et al.,* 2002; Rey *et al.,* 2005). *Hordeum vulgare* L. plants (cv. Express) were cultivated for 3 weeks as described in Marok *et al.,* (2013). All plants were cultivated in the "Phytotec" platform (CEA, DRF, BIAM).

Protein preparation

Leaves were ground in liquid nitrogen and the powder suspended in 50 mM Tris-HCl pH 8, 1 mM phenylmethylsulfonyl fluoride, PMSF, and 50 mM β-mercaptoethanol to prepare soluble proteins (Rey *et al*., 2005). In non-reducing conditions, the powder was suspended in 50 mM Tris-HCl pH 8 and 1 mM PMSF. Poly(vinylpolypyrrolidone), PVPP, was added in the extraction buffer (5%) when specified. Following vigorous shaking at 4°C for 20 min and centrifugation (20 min, 15,000 rpm, 4°C), the supernatant was precipitated using two volumes of acetone at -20°C and, when non-reduced, used rapidly for subsequent analyses. Protein concentration was quantified using the "Protein Quantification BCA Assay" kit (Interchim).

Alkylation experiments

Leaf soluble proteins were prepared in PBS pH 7.2, 1 mM PMSF in the absence of reductant and alkylated using mPEG-maleimide-2000 (Laysan Bio Arab, AL, USA) as reported in Rey *et al.,* (2017). Control experiments were performed on proteins extracted in the presence of 50 mM β-mercaptoethanol or 50 mM Tris(2-carboxyethyl)phosphine hydrochloride, TCEP). Proteins were precipitated using two acetone volumes at -20°C for 1 h and immediately used for labelling to approach the Cys redox status in a reliable manner. Following centrifugation, an aliquot of 200 µg protein was suspended in PBS pH 7.2, 1% SDS and 1.7 mg.mL^{-1} mPEG-maleimide-2000 and incubated at room temperature for 3 h. Then, the reaction mixture was added with loading buffer devoid or not of reductant for SDS-PAGE and Western blot analyses.

Electrophoresis and immunoblot analysis

Proteins were separated using SDS-PAGE in reducing or non-reducing conditions and electroblotted onto 0.45 µm nitrocellulose (Pall Corporation) to perform immunoblot analysis. Antibodies against hyperoxidized 2-CysPRX forms (Rabbit anti-peroxiredoxin-SO_3, reference

LF-PA0004) were purchased from AbFrontier (Seoul, Korea) and used at a dilution of 1:3,000. The At2-CysPRX antiserum was raised against the recombinant protein (Broin *et al.*, 2002) and used diluted 1:10,000. Bound antibodies were detected using either a goat anti-rabbit secondary antibody coupled to a fluorescent molecule at a dilution of 1:10,000 (Alexa Fluor 680, Invitrogen) using the 'Odyssey Infrared Imager' at 680 nm (Licor, Lincoln, NE, USA) or an anti-rabbit immunoglobulin G coupled to alkaline phosphatase (Sigma) for chromogenic detection. For assessing the level of hyperoxidation, membranes were probed first with the serum raised against hyperoxidized 2-CysPRX for fluorescent detection, and subsequently probed with the serum raised against At2-CysPRX for chromogenic detection. Quantification of band intensity was performed using the software associated with the imager.

Protein sequence and structure analysis

Sequence alignments were performed using the softwares "LALIGN" and "ClustalW" at the ExPASy resource portal. Protein structure predictions were done using the Phyre2 web portal (Kelley *et al.*, 2015). The best hit from the Phyre2 search carried out on the sequence of mature At2-CysPRXB and the mature Hv2-CysPRX was for both sequences the 3D structure of At2-CysPRXA C119S (PDB code 5ZTE) (Yang *et al.*, 2018) (96% alignment coverage (7-200aa), 100% confidence, 96% identity and 96% alignment coverage (8-201aa), 100% confidence, 93% identity, respectively). Structural comparisons and three-dimensional structure images were generated using PyMOL (PyMOL Molecular Graphics System, Version 2.0 Schrödinger, LLC).

Results

Variability of dimer/monomer distribution in plant 2-CysPRXs

Relatively few data are currently available regarding the plant 2-CysPRX dimer/monomer distribution that is revealed in non-reducing SDS-PAGE. We first analyzed by Western analysis the protein amount in Arabidopsis mutants deficient in one 2-CysPRX isoform (A or B), SRX or NTRC following extraction and migration in reducing conditions (Fig. 1A). The peroxidase was found almost exclusively as a 22-kDa monomer, the dimer band being faintly detected due to incomplete reduction. Compared to WT, the enzyme amount was not modified in *srx* plants as previously observed (Rey *et al.*, 2007), reduced by 25 to 30% in lines lacking 2-CysPRXB or NTRC and by *ca* 75% in the mutant lacking 2-CysPRXA. When extracted and migrated in the absence of reductant (Fig. 1B), 2-CysPRX appears as a monomer at 22 kDa and as a dimer at *ca* 45 kDa in WT extracts as previously reported

(Cerveau *et al.*, 2016*b*). Quantification of signal intensity revealed that in WT the monomer represents more than 50% of the total protein amount. A ratio in the same range was observed in lines lacking one PRX isoform or SRX. As observed by Pulido *et al.,* (2010) and Puerto-Galan *et al.,* (2015), this ratio was lower than 20% in *ntrc* plants due to a substantially lower monomer amount, clearly showing the decisive role of the electron donor in the maintenance of 2-CysPRX redox status.

Some data indicate that the dimer/monomer distribution of plant 2-CysPRXs could vary as a function of species. Indeed, a much lower monomer amount was observed in potato (Broin and Rey, 2003) compared to Arabidopsis (Baier and Dietz 1999; Cerveau *et al.,* 2016b). As this discrepancy might come from different preparation procedures, we compared the dimer/monomer distribution in extracts simultaneously and similarly prepared from Arabidopsis, potato and barley leaves. Of note, a lower 2-CysPRX total amount, was found in both cultivated species compared to Arabidopsis (Fig. 1C). In non-reducing conditions, the monomer proportion was much lower in barley (less than 20%) than in Arabidopsis and comparable to that in *ntrc* (Fig. 1D). Strikingly, this proportion was even lower in potato (less than 10%), the 22-kDa band being sometimes barely detected (Fig. 1D, data not shown) consistently with previous findings (Broin and Rey, 2003). When adding 5% polyvinylpolypyrrolidone in the extraction buffer to adsorb phenolic compounds, that are abundant in Solanaceae and promote oxidation of cell compounds, similar results were obtained (data not shown). These data highlight a strong variability in the 2-CysPRX dimer/monomer distribution among plant species.

Plant 2-CysPRX thiol content

The presence of free thiols in 2-CysPRX *in planta* is a parameter very likely underlying its peroxidase and/or signaling activities, which has not been thoroughly investigated so far. We analyzed the Cys redox status by carrying out alkylation experiments using mPEG-maleimide-2000, which forms stable thioether bonds with thiol groups, allowing the detection of reduced Cys due to a 2-kDa size increase per free thiol. Following incubation with this compound in the absence of reductant and Western analysis, 2-CysPRX bands displaying slower mobility were specifically revealed in WT compared to *2-cysprxa 2-cysprxb* (Fig. 2A). One additional monomer band at *ca* 25 kDa and another faint one at *ca* 23.5 were observed. Regarding dimer, one supplementary band at *ca* 48 kDa and another higher faint band were detected. We then performed the same experiments using protein extracts from mutants deficient in one 2-CysPRX, SRX or NTRC (Fig. 2A). We did not observe any qualitative

difference in the alkylation patterns compared to WT, except in *ntrc* where no higher monomer band was detected due to the very low abundance of the 22-kDa form in this genotype (Fig. 2A).

The patterns in non-reducing conditions did not allow accurately determining the number of free thiols in 2-CysPRX monomers or dimers, notably due to the presence of several bands in non-alkylated extracts. To better approach this parameter, alkylated WT samples prepared in non-reducing conditions were subjected to SDS-PAGE in the presence of reductant (Fig. 2B). No dimer was detected as expected and one supplementary band at *ca* 25 kDa was observed compared to non-alkylated samples. The intensity of this band was low compared to that revealed in reduced non-alkylated extracts (Fig. 2B, lanes 1 and 3). As a control, we analyzed the number of free thiols in 2-CysPRX using protein extracts prepared directly in reducing conditions in the presence of β-mercaptoethanol. The revelation pattern was very similar to that obtained using oxidized proteins, but with a higher intensity of the supplementary 25-kDa band (Fig. 2B, lanes 1-2). This is consistent with the fact that dimer reduction leads to the appearance of free thiols available for alkylation. Nonetheless, the intensity of this band remained lower than that of the 22-kDa isoforms. When using extracts from *ntrc* or *srx* plants (Fig. 2B, lanes 4-9), very similar data were obtained, indicating that the absence of one of these two 2-CysPRX partners does not substantially alter the protein thiol content.

Two Cys residues are present in the sequence of mature 2-CysPRX. The appearance of only one supplementary alkylated band, even in extracts reduced using β-mercaptoethanol, raised questions and prompted us to use another reductant. TCEP, tris(2-carboxyethyl)phosphine) is a powerful non-thiol reductant, compared to DTT and β-mercaptoethanol, that proved more appropriate for Cys labeling with maleimides, since it is less deleterious to conjugation with these compounds (Getz *et al*., 1999). Reduction by TCEP led to a very distinct pattern compared to that observed with β-mercaptoethanol. Indeed, a very intense 28-kDa band was revealed, while the previously detected 25-kDa band was still present and the bands at *ca* 22 kDa almost absent (Fig. 2C, lane 3). The appearance of two major bands shifted by *ca* 2.5 and 5 kDa, is consistent with the presence of two free thiols in reduced 2-CysPRX that can be alkylated only in the presence of TCEP. These data lead us to conclude that since only the 25-kDa alkylated band is revealed in proteins prepared in non-reducing conditions, 2-CysPRX from leaf extracts probably harbors only one reduced Cys residue. Further, the lower intensity of this band compared to those at 22 kDa suggests that a limited protein fraction carries one free thiol. Alkylation experiments were finally carried out

on leaf extracts from barley and potato. In non-reduced extracts, a lower intensity of the additional 25-kDa band was noticed in both species compared to Arabidopsis (Fig. 2D, lanes 1, 4 and 7). Following alkylation of TCEP-reduced extracts, two major bands at *ca* 25 and 28 kDa were revealed. Note that the abundance of the 25-kDa band appeared much higher in barley and potato than in Arabidopsis (Fig. 2D, lanes 2, 5 and 8). Altogether, these data suggest that in leaf extracts only a limited 2-CysPRX pool harbors one reduced Cys.

Redox status of 2-CysPRX as a function of light cycle in Arabidopsis.

2-CysPRXs fulfill a key role in the regulation of photosynthesis upon the light-dark transition (Yoshida *et al*., 2018). In other respects, 2-CysPRX hyperoxidation follows a circadian rhythm (O'Neill *et al*., 2011; Cerveau *et al.*, 2016*b*). Therefore, we investigated whether the dimer/monomer distribution and the proportion of protein carrying one free thiol varies as a function of light cycle. Arabidopsis WT leaves were collected at five time points (Fig. S1): before and after the dark-light transition (D1 and L1, respectively), middle of the light period (L2), before and after the light-dark transition (L3 and D2, respectively). No change was observed in the total 2-CysPRX abundance while a substantially higher amount of the hyperoxidized form was detected following the dark-light transition and at the middle of the light period (Fig. 3A). In the absence of reductant, the amounts of both dimer and monomer forms in WT noticeably decreased along the light period, the lowest ones being observed after the light-dark transition (Fig. 3B). Quantification of band intensities indicated that the 2-CysPRX amount detected as both monomer and dimer forms was decreased by more than 25% at the D2 time point compared to L1 (Fig. 3C). Similar data were obtained when analyzing *srx* proteins (Fig. 3D). In *ntrc*, where the monomer amount is very low, the dimer abundance decreased along the light phase and the monomer amount slightly increased following the dark-light transition and then decreased (Fig. 3D). Finally, we performed alkylation experiments on WT leaf extracts collected at the five time points and prepared without reductant. No noticeable variation in the abundance of the supplementary 25-kDa band was observed as a function of light phase (Fig. 3E). In *ntrc* alkylated extracts, a slight increase in the abundance of the 25-kDa band was noticed before the light-dark transition (Fig. S2). Altogether, these data reveal that light cycle in addition to regulating hyperoxidation, strongly influences the 2-CysPRX amount detected in the range from 20 to 50 kDa in non-reducing conditions, while it does not provoke any substantial change in the total protein amount and thiol content.

Redox status of 2-CysPRX as a function of light cycle in barley and potato.

We then investigated the effect of light cycle on 2-CysPRX redox status in barley and potato. In the presence of reductant, no change was observed regarding the protein abundance in both species (Fig. 4A-B). In barley, similarly to what observed in Arabidopsis, we noticed a strong increase in the amount of the hyperoxidized form following the dark-light transition and a noticeable decrease at the beginning of the dark phase (Figs. 3A, 4A). A distinct pattern was noticed in potato, since the highest amounts of hyperoxidized 2-CysPRX were observed before and following the light phase (Fig. 4B). In non-reducing conditions, a low amount of 2-CysPRX monomer was detected in both species as shown above (Figs. 1D, 4C-D). In barley, the dimer abundance slightly decreased during the light period, the lowest amount being observed at the beginning of the dark phase, while a substantially higher monomer abundance was observed at the middle of the light period (Fig. 4C). In potato, a gradual decrease in the dimer amount was observed along the light period, the lowest amount being noticed at the beginning of the dark phase. Of note, a noticeably higher monomer abundance was revealed at the end of the light period (Fig. 4D). Alkylation experiments revealed no change in the abundance of the supplementary 25-kDa band in both species as a function of light cycle (Fig. 4E-F).

Redox status of 2-CysPRX in potato lines modified for *CDSP32* expression

We previously generated potato lines modified for the expression of the CDSP32 TRX that interacts with 2-CysPRX and reduces it (Broin *et al.*, 2002; Broin and Rey, 2003). Here, we analyzed the redox status of 2-CysPRX in lines co-suppressed (CS), or over-expressing WT (OE) or active-site mutated (OE-M) CDSP32. In all lines, a similar peroxidase abundance was found (Fig. 5A). We noticed that the CDSP32-deficient line exhibits the lowest level of hyperoxidized PRX (Fig. 5A) as already observed (Cerveau *et al*., 2016*b*). In non-reducing conditions, plants co-suppressed for *CDSP32* displayed a higher monomer amount than WT (Fig. 5B) as reported in Broin and Rey (2003). Consistently, the lowest monomer level was observed in the line over-expressing *CDSP32*. Of note, both lines expressing a CDSP32 form lacking CysP displayed a monomer abundance noticeably higher than that in plants overexpressing the WT TRX. Finally, we examined the 2-CysPRX thiol content by performing alkylation experiments. As observed in Figs. 2D and 4F, a very low abundance of the 25-kDa additional band was detected in WT (Fig. 5C). However, a higher band intensity was noticed in all lines modified for *CDSP32* expression, particularly CS and OE-M,

indicating that the absence of functional CDSP32 is associated with an increased thiol content in 2-CysPRX.

Differential behavior of plant 2-CysPRXs towards hyperoxidation

Finally, we investigated whether plant 2-CysPRXs exhibit variability regarding hyperoxidation as observed for human 2-CysPRXs. We first compared the amount of 2-CysPRXs A and B in young, adult and old leaves of Arabidopsis WT and mutants deficient in one of the two isoforms (Fig. 6A). 2-CysPRXs A and B were found to account for *ca* 75% and 25 % of the WT level whatever the developmental stage (Fig. 6B) in agreement with Kirchsteiger *et al.,* (2009). No variation in protein abundance was observed as a function of leaf age in the three genotypes. We previously reported that 2-CysPRX hyperoxidation level decreases with leaf age in WT (Cerveau *et al.,* 2016*b*). The age-dependent hyperoxidation pattern in plants expressing only *2-CysPRXA* was very similar to that observed in WT. In contrast, only a faint band corresponding to hyperoxidized 2-CysPRXB vas detected in young leaves of *2-cysprxa* plants, and this form was not revealed in old leaves (Fig. 6A). Quantification revealed that hyperoxidized 2-CysPRXB in young, adult and old leaves represents 10, 3 and 0%, respectively, of that in WT, whereas this isoform represents 25 to 30% of the total protein amount (Fig. 6B). Consistently, the level of hyperoxidized 2-CysPRXA reaches values in the range of 100% of those in WT at all developmental stages. These data indicate that At2-CysPRXB is substantially less prone to hyperoxidation than At2-CysPRXA. We then compared the abundance of the hyperoxidized form in Arabidopsis, barley and potato. In reducing conditions, a similar 2-CysPRX amount, lower than that in Arabidopsis, was noticed in both cultivated species (Figs. 6C, 1C). Strikingly, a much higher abundance of the hyperoxidized form was observed in barley compared to Arabidopsis and potato, revealing a higher sensitivity in this species (Fig. 6C).

We thus searched for the sequence determinants possibly underlying the differential behavior of At2-CysPRXB and Hv2-CysPRX within or in the proximity of the motifs A and B that are involved in hyperoxidation resistance (Bolduc *et al.*, 2018). When aligning the four sequences (Fig. 7A), we observed very few differences, but noticed that an Ile residue instead of Val just precedes the motif B in At2-CysPRXB. Regarding the sequence of Hv2-CysPRX, two residues in the motif A differ compared to the other PRXs (Ile-136 and Lys-164 instead of Val and Asn, respectively). These two residues, which exhibit different steric hindrance or charge, are located in close vicinity of the CysP residue, the GGLG motif and the dimer-dimer interface (Bolduc *et al.,* 2018). Within the 3D Phyre2 model of Hv2-CysPRX, Ile 136

and Lys-164 are also close to each other (distance between 7.5 to 10 Å) (Figs. 7B-C). Furthermore, structural comparison between the 3D structure of At2-CysPRXA C119S (PDB code 5ZTE) (Yang *et al.*, 2018) and the 3D model of Hv2-CysPRX shows that the two residue differences within motif A induce electrostatic surface potential changes very close to the GGLG motif.

Discussion

Plant 2-CysPRXs display a high abundance and limited variations in gene expression in relation to developmental factors and environmental constraints (Broin and Rey, 2003; Dietz *et al.*, 2006; Cerveau *et al*., 2016*b*). Comparatively, more important variations were observed regarding hyperoxidation level or quaternary structure (Broin and Rey, 2003; König *et al*., 2003; Cerveau *et al*., 2016*b*). The present report provides new information particularly regarding protein hyperoxidation, thiol content and dimer/monomer distribution in relation with light cycle, but also species type.

Plant 2-CysPRX hyperoxidation

In eukaryotic organisms, 2-CysPRX hyperoxidation follows a circadian rhythm while no change occurs in transcription rate and protein amount (O'Neil *et al*., 2011; Edgar *et al*., 2012). In Arabidopsis, our previous data (Cerveau *et al.*, 2016*b*) and this work (Fig. 3A) reveal higher levels of hyperoxidation following the dark-light transition. A similar pattern was observed in barley, but in potato the highest level was noticed after the light-dark transition (Fig. 4A-B). Arabidopsis and barley were cultivated under short photoperiod and potato under longer day length, raising the question of the influence of this parameter. When examining 2-CysPRX hyperoxidation in Arabidopsis plants grown under a 16-h photoperiod, Puerto-Galan *et al.*, (2015) observed a higher level following the dark-light transition. Lastly, Edgar *et al.*, (2012) showed persistent oscillations of hyperoxidation in Arabidopsis seedlings grown under a 12-h photoperiod and then exposed to continuous light, the highest levels occurring at Zeitgeber time points corresponding to the beginning of the light phase. These data indicate that in Arabidopsis 2-CysPRX hyperoxidation peaks following the dark-light transition whatever the photoperiod length. However, as shown in potato, such a pattern cannot be extended to all plant species.

Eukaryote 2-CysPRXs exhibit two motifs (GGLG and YF) considered as a signature of hyperoxidation sensitivity (Wood *et al.*, 2003). However, human 2-CysPRXs 1, 2 and 3 exhibit differential susceptibility to hyperoxidation (Cox *et al.*, 2009). The higher resistance

of human PRX3 is linked to the presence of the two motifs A and B also found in bacterial 2-Cys PRXs (Bolduc *et al.*, 2018). Interestingly, plant 2-CysPRXs display both motifs A and B (Fig. 7), but still exhibit differential susceptibility to hyperoxidation, as clearly shown for At2-CysPRXB and Hv2-CysPRX, which are less and more sensitive to this redox modification, respectively (Fig. 6). This differential behavior might be linked to sequence differences within or in the proximity of motifs A and B (Fig. 7A). Plant 2-CysPRXs are highly conserved and differ by only a limited number of residues (Fig. 7A). Interestingly an Ile residue, instead of Val in the three other proteins, precedes the motif B in At2-CysPRXB. Structural comparison between the 3D structure of At2-CysPRXA C119S and the 3D model of At2-CysPRXB shows that this Ile, which has a higher steric hindrance, is located between motif A and B (Fig. S3). This modification could explain the better resistance of At2-CysPRXB to hyperoxidation, and this residue could be included in the motif B. Concerning the barley enzyme, that shows a higher level of sensitivity, its motif A contains two specific residues (Ile-136 and Lys-164) that induce electrostatic surface changes very close to the GGLC motif (Figs. 7B-C). This modification could alter the property of this motif, which is a key determinant in hyperoxidation sensitivity. A survey of motifs A and B in various plant 2-CysPRXs reveals even more sequence divergence within these two motifs, notably in the first part of motif A, which is associated with the α helix leading to CysP, and regarding the last residue in motif B that can also be an Ala instead of Ser in some species (Fig. S4). Based on these findings, we propose that such variations in motifs A and B fine-tune differential hyperoxidation in plant 2-CysPRXS (Fig. 8) and confer them distinct physiological functions. Indeed, hyperoxidation results in inactivation of peroxidase activity and initiation of signaling responses (Wood *et al*., 2003; Rey *et al*., 2007; Bolduc *et al.*, 2018). Up to now, no data support distinct functions since Arabidopsis mutants deficient in one 2-CysPRX do not exhibit any obvious phenotype in standard conditions (Kirchsteiger *et al*., 2009). Further investigations in challenging conditions are thus needed. Finally, we can also hypothesize that the subtle sequence divergence among plant 2-Cys PRXs underlie specific structural features, such as the dimer/monomer distribution, as observed in Arabidopsis and potato (Fig. 1D).

Thiol content in plant 2-CysPRXs

The content in free thiols is likely a critical determinant underlying 2-CysPRX functions. Very few data are available regarding this parameter even outside the plant kingdom. By performing alkylation experiments on leaf proteins, we show that a minor proportion of the peroxidase displays shifted migration to 25 kDa (Fig. 2). This *ex vivo* approach suggests that

only a limited pool of 2-CysPRX carries one free thiol in leaf cells. Perez-Ruiz *et al.*, (2017), when performing alkylation experiments using methyl-maleimide polyethylene glycol24 on Arabidopsis extracts, observed the appearance of one major upper band and another very faint one very close in size to the latter. These two bands were attributed to 2-CysPRX forms harboring one or two free thiols. However, no marker size and no control on fully reduced proteins were shown to unambiguously identify the one- and two-free-thiol forms. When carefully examining and comparing the pattern from Fig. 2C to that reported by Perez-Ruiz *et al.*, (2017), it seems that the two very close bands revealed by this group might correspond to one unique alkylated form. The high proportion of oxidized Cys in 2-CysPRX observed here is in agreement with the conclusion of Vaseghi *et al.*, (2018), which was based on the monomer abundance in Arabidopsis extracts migrated in non-reducing conditions. To perform peroxidase activity, typical 2-CysPRXs assemble in obligate homodimers that are presumed to be reduced or bound with one or two disulfide bounds (Dietz, 2011). Our experiments revealed that most Cys are oxidized (Fig. 2), indicating that a high proportion of dimers likely display two disulfide bounds. Of note, the abundance of the alkylated 25-kDa band was found higher in Arabidopsis than in barley and potato (Fig. 2D). Since the protein is revealed mainly as a dimer in non-reducing SDS-PAGE in the two cultivated species compared to Arabidopsis (Fig. 1D), we might infer that dimer forms are bound by two disulfide bridges and that there is a positive relationship between the monomer amount and the presence of free thiols in 2-CysPRX, as hypothesized by Vaseghi et *al.*, (2018).

In the three species studied, no substantial change was observed in the amount of the additional 25-kDa band along the light cycle (Figs. 3E, 4E-F). Consistently, Perez-Ruiz *et al*., (2017) reported no variation in the alkylation pattern following the dark-light transition in WT Arabidopsis. However, the abundance of this band increased in *ntrc* at the beginning of the light period (Perez-Ruiz *et al.*, 2017). In our experiments, we noticed increased intensity of the 25-kDa alkylated band in *ntrc* at the end of the light phase (Fig. S1). Moreover, potato plants lacking the CDSP32 TRX or those expressing a non-active form exhibit a higher abundance of the 2-CysPRX form carrying one free thiol (Fig. 5C), further highlighting the importance of reductants in the maintenance of 2-CysPRX thiol content.

Relationship between 2-CysPRX redox status, quaternary structure and functions

2-CysPRXs display several quaternary structures such as monomer, dimer and HMW complexes including tetramer and decamer (Dietz, 2011; Cerveau *et al.*, 2016*b*). Of note, the monomer level revealed by SDS-PAGE in the absence of reductant is non-representative of

the original level, partly due to SDS dissociation of non-covalently bound forms. Nonetheless, this migration feature is a valuable indicator of protein structure and reveals a striking species-dependent variability. Surprisingly, a very low monomer abundance was recorded in potato and barley (König *et al.,* 2002; Broin and Rey, 2003; König *et al.,* 2003) while a much higher amount was noticed in Arabidopsis and tomato (Baier and Dietz 1999; Cerveau *et al* 2016*b*; Puerto-Galan *et al.,* 2015; Pulido *et al.,* 2010; Xia *et al.,* 2018). When preparing proteins from Arabidopsis, barley and potato in a simultaneous and similar manner, we get results highly consistent to those reported in the literature *i.e.* a monomer proportion of *ca* 50% in Arabidopsis and lower than 20% in the two other species (Fig. 1B). We thus conclude that the 2-CysPRX dimer/monomer distribution revealed in non-reducing SDS-PAGE strongly depends on species type. This feature might be an indicator of preferential PRX functions among the plant kingdom.

Based on Arabidopsis data, Puerto-Galan *et al.,* (2015) and Cerveau *et al.,* (2016*b*) concluded to a correlation between hyperoxidation level and monomer abundance in non-reducing SDS-PAGE. However, barley is characterized by a low monomer amount and a much higher abundance of hyperoxidized enzyme (Figs. 6C, 1D) and potato plants co-suppressed for *CDSP32* concomitantly display compared to other lines the highest monomer level and the lowest amount of hyperoxidized protein (Fig. 5 A-B). This clearly demonstrates the absence of relationship between plant 2-CysPRX monomer abundance and hyperoxidation level. Of note, the absence of reductants such as NTRC in Arabidopsis and CDSP32 in potato is associated with altered dimer to monomer proportion (Figs. 1B, D; 5B), highlighting the importance of physiological reductants in the maintenance of enzyme quaternary structure. Within a species, the dimer/monomer ratio could be a marker of proper redox homeostasis. Indeed, potato plants modified for *CDSP32* expression exhibit no phenotype in standard conditions, but increased sensitivity to oxidative stress (Broin *et al.,* 2002; Rey *et al.,* 2005).

In other respects, the 2-CysPRX distribution in dimer and monomer forms is very likely related to environmental conditions. Indeed, a higher monomer proportion was observed in potato and barley upon osmotic or oxidative constraints (König *et al*., 2002; Broin and Rey, 2003), and this proportion decreased in tomato in response to chilling (Xia *et al.,* 2018). Further evidence of environment influence on monomer and dimer distribution is deduced from the patterns along the light cycle. In barley, the monomer amount is substantially higher during the light period and in potato, the highest amount is recorded at the end of the light phase (Fig. 4 C-D). Intriguingly in WT Arabidopsis, the protein detected as both dimer and monomer in the 20-50 kDa range in non-reducing conditions is 25% lower at the beginning of

the dark period compared to the beginning of the light phase (Fig. 3C). Similar data were observed in *ntrc* and *srx* mutants (Fig. 3D) and in potato (Fig. 4D). In barley, no such a change was noticed, but the monomer amount substantially decreased following the light-dark transition (Fig. 4C). The variations observed in Arabidopsis and potato appear at first sight contradictory to the patterns in reducing conditions, since no change in the total protein abundance occurs depending on light cycle (Figs. 3A, 4A-B). This discrepancy might originate from 2-CysPRX involvement in HMW complexes or covalent binding to partners. The enzyme is indeed susceptible to interact with numerous partners as reported in Arabidopsis (Cerveau *et al.*, 2016*a*). These homo- or heteromeric complexes could be poorly detected by antibodies or migrate outside the 20-100 kDa gel area. Thus, we can presume that 2-CysPRX binding occurs at specific time points, such as at the end of the light phase, where this enzyme fulfills a critical role in re-oxidation of TRXs and deactivation of photosynthetic enzymes (Yoshida *et al*., 2014; Yoshida *et al*., 2018).

The data presented here reveal a striking complexity of 2-CysPRX hyperoxidation level and quaternary structure that depend on environmental factors such as light cycle, but also on species. In contrast, the low thiol content observed in three species does not vary along the light cycle, indicating that most of the 2-CysPRX pool is oxidized. This enzyme, which is considered as a major plastidial regulatory hub (Muthuramalingam *et al.,* 2009), could play a role of oxidant buffer allowing the maintenance of proper plastidial redox homeostasis in concert with diverse TRX types (Vieira Dos Santos and Rey, 2006) depending on physiological context (Broin *et al.,* 2002; Perez-Ruiz *et al.,* 2006; Dangoor *et al.,* 2012 ; Eliyahu *et al.,* 2015; Yoshida *et al.,* 2018). For instance, the function of photosynthesis deactivation during the light-dark transition would be ensured via the dimer peroxidase activity and subsequent regeneration by the atypical TRX-like2 (Yoshida *et al.,* 2018). But, oxidized 2-CysPRX could also directly interact with reduced non-TRX partners as inferred from the Arabidopsis PRX interactome (Cerveau *et al.,* 2016*a*) and the capacity of the human ezyme to oxidize proteins (Stocker *et al.,* 2017). Finally, the other oxidized PRX forms, such as hyperoxidized monomer, are very likely involved in sensing and transmitting redox information (Liebthal *et al.,* 2018) in relation for instance with light cycle. This signal could be transduced via the control of peroxide concentration as proposed in the floodgate theory (Poole *et al.,* 2011) or interaction with specific partners remaining to be identified.

Acknowledgements: We are very grateful to the “Phytotec” platform (CEA, DRF, BIAM) for technical assistance with growth chambers and to Prof N. ROUHIER (Université de Lorraine) for valuable discussion. D. Cerveau acknowledges financial support for a PhD grant (DEB 12-1538) from the “Région Provence-Alpes-Côte d’Azur”.

References

Awad J, Stotz HU, Fekete A, Krischke M, Engert C, Havaux M, Berger S, Mueller MJ. 2015. 2-Cys peroxiredoxins and thylakoid ascorbate peroxidase create a water-water cycle that is essential to protect the photosynthetic apparatus under light stress conditions. Plant Physiology **167**, 1592-603.

Baier M, Dietz KJ. 1996. Primary structure and expression of plant homologues of animal and fungal thioredoxin-dependent peroxide reductases and bacterial alkyl hydroperoxide reductases. Plant Molecular Biology **31**, 553-564.

Baier M, Dietz KJ. 1997. The plant 2-Cys peroxiredoxin BAS1 is a nuclear-encoded chloroplast protein: its expressional regulation, phylogenetic origin, and implications for its specific physiological function in plants. The Plant Journal **12**, 179-190.

Baier M, Dietz KJ. 1999. Protective function of chloroplast 2-cysteine peroxiredoxin in photosynthesis. Evidence from transgenic Arabidopsis. Plant Physiology **119**,1407-1414.

Biteau B, Labarre J, Toledano MB. 2003. ATP-dependent reduction of cysteine-sulphinic acid by *S. cerevisiae* sulphiredoxin. Nature **425**, 980-984.

Bolduc JA, Nelson KJ, Haynes AC, Lee J, Reisz JA, Graff AH, Clodfelter JE, Parsonage D, Poole LB, Furdui CM, Lowther WT. 2018. Novel hyperoxidation resistance motifs in 2-Cys peroxiredoxins. The Journal of Biological Chemistry **293**, 11901-11912.

Broin M, Rey P. 2003. Potato plants lacking the CDSP32 plastidic thioredoxin exhibit hyperoxidation of the BAS1 2-Cysteine peroxiredoxin and increased lipid peroxidation in thylakoids under photooxidative stress. Plant Physiology **132**, 1335-1343.

Broin M, Cuiné S, Eymery F, Rey P. 2002. The plastidic 2-Cystein peroxiredoxin is a target for a thioredoxin involved in the protection of the photosynthetic apparatus against oxidative stress. The Plant Cell **14,** 1417-1432.

Cerveau D, Kraut A, Stotz HU, Mueller MJ, Couté Y, Rey P. 2016*a*. Characterization of the *Arabidopsis thaliana* 2-Cys peroxiredoxin interactome. Plant Science **252**, 30–41.

Cerveau D, Ouahrani D, Marok MA, Blanchard L Rey P. 2016*b*. Physiological relevance of plant 2-Cys peroxiredoxin overoxidation level and oligomerization status. Plant Cell & Environment **39**, 103–119.

Coic Y, Lesaint C. 1971. Comment assurer une bonne nutrition en eau et ions minéraux en horticulture. Horticulture Française **8**, 11-14.

Collin V, Issakidis-Bourguet E, Marchand C, Hirasawa M, Lancelin JM, Knaff DB, Miginiac-Maslow M. 2003. Enzyme catalysis and regulation: the *Arabidopsis* plastidial thioredoxins: new functions and new insights into specificity. The Journal of Biological Chemistry **278**, 23747-23752.

Cox AG, Pearson AG, Pullar JM, Jönsson TJ, Lowther WT, Winterbourn CC, Hampton MB. 2009. Mitochondrial peroxiredoxin 3 is more resilient to hyperoxidation than cytoplasmic peroxiredoxins. Biochemical Journal **421**, 51-58.

Dangoor I, Peled-Zehavi H, Wittenberg G, Danon A. 2012. A chloroplast light-regulated oxidative sensor for moderate light intensity in Arabidopsis. The Plant Cell **24**, 1894-1906.

Day AM, Brown JD, Taylor SR, Rand JD, Morgan BA, Veal EA. 2012. Inactivation of a peroxiredoxin by hydrogen peroxide is critical for thioredoxin-mediated repair of oxidized proteins and cell survival. Molecular Cell **45**, 398-408.

Dietz KJ. 2011. Peroxiredoxins in plants and cyanobacteria. Antioxidant & Redox Signaling **15**, 1129-1159.

Dietz KJ, Jacob S, Oelze ML, Laxa M, Tognetti V, Marina S, de Miranda N, Baier M, Finkemeier I. 2006. The function of peroxiredoxins in plant organelle redox metabolism. Journal of Experimental Botany **57**, 1697–1709.

Edgar RS, Green EW, Zhao Y, van Ooijen G, Olmedo M, Qin X, Xu Y, Pan M, Valekunja UK, Feeney KA, Maywood ES, Hastings MH, Baliga NS, Merrow M, Millar AJ, Johnson CH, Kyriacou CP, O'Neill1 J.S, Reddy AB. 2012. Peroxiredoxins are conserved markers of circadian rhythms. Nature **485**, 459-467.

Eliyahu E, Rog I, Inbal D, Danon A. 2015. ACHT4-driven oxidation of APS1 attenuates starch synthesis under low light intensity in Arabidopsis plants. Proceedings of the National Academy of Sciences of the United States of America, **112,** 12876-12881.

Gama F, Brehelin C, Gelhaye E, Meyer Y, Jacquot JP, Rey P, Rouhier N. 2008. Functional analysis and expression characteristics of chloroplastic Prx IIE. Physiologia Plantarum **133**, 599-610.

595 **Getz EB, Xiao M, Chakrabarty T, Cooke R, Selvin PR.** 1999. A comparison between the
596 sulfhydryl reductants tris2-carboxyethyl.phosphine and dithiothreitol for use in protein
597 biochemistry. Analytical Biochemistry **273**, 73-80

598 **Haynes AC, Qian J, Reisz JA, Furdui CM, Lowther WT.** 2013. Molecular basis for the
599 resistance of human mitochondrial 2-Cys peroxiredoxin 3 to hyperoxidation. The Journal of
600 Biological Chemistry**288**, 29714-29723.

601 **Jang HH, Lee KO, Chi YH, Jung BG, Park SK, Park JH, Lee JR, Lee SS, Moon JC,**
602 **Yun JW, Choi YO, Kim WY, Kang JS, Cheong GW, Yun DJ, Rhee SG, Cho MJ, Lee**
603 **SY.** 2004. Two enzymes in one: two yeast peroxiredoxins display oxidative stress-dependent
604 switching from a peroxidase to a molecular chaperone function. Cell **117**, 625-635.

605 **Jönsson TJ, Murray MS, Johnson LC, Lowther WT.** 2008. Reduction of cysteine sulfinic
606 acid in peroxiredoxin by sulfiredoxin proceeds directly through a sulfinic phosphoryl ester
607 intermediate. The Journal of Biological Chemistry **283**, 23846-23851.

608 **Kelley LA, Mezulis S, Yates CM, Wass MN, Sternberg MJ.** 2015. The Phyre2 web portal
609 for protein modeling, prediction and analysis. Nature Protocols **10**, 845-858.

610 **Kim IH, Kim K, Rhee SG.** 1989. Induction of an antioxidant protein of *Saccharomyces*
611 *cerevisiae* by O_2, Fe^{3+}, or β-mercaptoethanol. Biochemistry **86**, 6018-6022.

612 **Kirchsteiger K, Pulido P, González M, Cejudo J.** 2009. NADPH thioredoxin reductase C
613 controls the redox status of chloroplast 2-Cys peroxiredoxins in *Arabidopsis thaliana*.
614 Molecular Plant **2**, 298-307.

615 **König J, Baier M, Horling F, Kahmann U, Harris G, Schürmann, Dietz KJ.** 2002. The
616 plant-specific function of 2-Cys peroxiredoxin-mediated detoxification of peroxides in the
617 redox-hierarchy of photosynthetic electron flux. Proceedings of the National Academy of
618 Sciences of the United States of America **99**, 5738-5743.

619 **König J, Lotte K, Plessow R, Brockhinke A, Baier M, Dietz KJ.** 2003. Reaction
620 mechanism of plant 2-Cys peroxiredoxin. Role of the C terminus and the quaternary structure.
621 The Journal of Biological Chemistry **278**, 24409-24420.

622 **Lamkemeyer P, Laxa M, Collin V, Li W, Finkemeier I, Schöttler MA, Holtkamp V,**
623 **Tognetti VB, Issakis-Bourguet E, Kandlbinder A, Weis E, Miginiac-Maslow M, Dietz**

KJ. 2006. Peroxiredoxin Q of Arabidopsis thaliana is attached to the thylakoids and functions in context of photosynthesis. The Plant Journal **45**, 968-981.

Lepisto A, Kangasjärvi S, Luomala EM, Brader G, Sipari N, Keränen M, Keinänen M, Rintamäki E. 2009. Chloroplast NADPH-thioredoxin reductase interacts with photoperiodic development in Arabidopsis. Plant Physiology **149**, 1261-1276.

Liebthal M, Maynard D, Dietz KJ. 2018. Peroxiredoxins and redox signaling in plants. Antioxidants & Redox Signaling **28,** 609-624.

Liu XP, Liu XY, Zhang J, Xia ZL, Liu X, Qin HJ, Wang DW. 2006. Molecular and functional characterization of sulfiredoxin homologs from higher plants. Cell Research **16**, 287-296.

Marok MA, Tarrago L, Ksas B, Henri P, Abrous-Belbachir O, Havaux M, Rey P. 2013. A drought-sensitive barley variety displays oxidative stress and strongly increased contents in low-molecular weight antioxidant compounds during water deficit compared to a tolerant variety. Journal of Plant Physiology **170**, 633-645.

Moon JC, Jang HH, Chae HB, Lee JR, Lee SY, Jung YJ, Shin MR, Lim HS, Chung WS, Yun DJ, Lee KO, Lee SY. 2006. The C-type *Arabidopsis* thioredoxin reductase ANTR-C acts as an electron donor to 2-Cys peroxiredoxins in chloroplasts. Biochemical and Biophysical Research Communications **348**, 478-484.

Muthuramalingam M, Seidel T, Laxa M, Nunes de Miranda SM, Gärtner F, Ströher E, Kandlbinder A, Dietz KJ. 2009. Multiple redox and non-redox interactions define 2-Cys peroxiredoxin as a regulatory hub in the chloroplast. Molecular Plant **2**, 1273-1288

Ojeda V, Pérez-Ruiz JM, Cejudo FJ. 2018. 2-Cys peroxiredoxins participate in the oxidation of chloroplast enzymes in the dark. Molecular Plant **11**, 1377-1388.

O'Neill J, Van Ooijen G, Dixon LE, Troein C, Corellou F, Bouget FY, Reddy AB, Millar AJ. 2011. Circadian rhythms persist without transcription in a eukaryote. Nature **469**, 554-558.

Perez-Ruiz JM, Cejudo FJ. 2009. A proposed reaction mechanism for rice NADPH thioredoxin reductase C, an enzyme with protein disulfide reductase activity. FEBS Letters **583**, 1399-1402.

Pérez-Ruiz JM, Naranjo B, Ojeda V, Guinea M, Cejudo FJ. 2017. NTRC-dependent redox balance of 2-Cys peroxiredoxins is needed for optimal function of the photosynthetic apparatus. Proceedings of the National Academy of Sciences of the United States of America **114**, 12069-12074

Perez-Ruiz JM, Spınola MC, Kirchsteiger K, Moreno J, Sahrawy M, Cejudo FJ. 2006. Rice NTRC is a high-efficiency redox system for chloroplast protection against oxidative damage. The Plant Cell **18**, 2356–2368.

Poole LB, Hall A, Nelson KJ. 2011. Overview of peroxiredoxins in oxidant defense and redox regulation. Current Protocols in Toxicology **49,** 7.9, 7.9.1–7.9.15.

Puerto-Galan L, Perez-Ruiz JM, Guinea M, Cejudo FJ. 2015. The contribution of NADPH thioredoxin reductase C (NTRC) and sulfiredoxin to 2-Cys peroxiredoxin overoxidation in *Arabidopsis thaliana* chloroplasts. Journal of Experimental Botany **66,** 2957-2966.

Pulido P, Spınola MC, Kirchsteiger K, Guinea M, Pascual MB, Sahrawy M, Sandalio LM, Dietz KJ, Gonzalez M, Cejudo FJ. 2010. Functional analysis of the pathways for 2-Cys peroxiredoxin reduction in *Arabidopsis thaliana* chloroplasts. Journal of Experimental Botany **61**, 4043-4054.

Rey P, Becuwe N, Barrault MB, Rumeau D, Havaux M, Biteau B, Toledano MB. 2007. The *Arabidopsis thaliana* sulfiredoxin is a plastidic acid reductase involved in the photooxidative stress response. The Plant Journal **49**, 505-514.

Rey P, Becuwe N, Tourrette S, Rouhier N. 2017. Involvement of Arabidopsis glutaredoxin S14 in the maintenance of chlorophyll content Plant Cell & Environment **40**, 2319–2332.

Rey P, Cuiné S, Eymery F, Garin J, Court M, Jacquot JP, Rouhier N, Broin M. 2005. Analysis of the proteins targeted by CDSP32, a plastidic thioredoxin participating in oxidative stress responses. The Plant Journal **41**, 31-42.

Rey P, Pruvot G, Becuwe N, Eymery F, Rumeau D, Peltier G. 1998. A novel thioredoxin-like protein located in the chloroplast is induced by water deficit in *Solanum tuberosum* L. plants. The Plant Journal **13**, 97–107.

Rhee SG. 2016. Overview on Peroxiredoxin. Molecules and Cells **39**, 1-5.

Rhee SG, Woo HA. 2011. Multiple functions of peroxiredoxins: peroxidases, sensors and regulators of the intracellular messenger H_2O_2 and protein chaperones. Antioxidant & Redox Signaling **15**, 781-794.

Serrato AJ, Perez-Ruiz JM Spinola MC, Cejudo FJ. 2004. A novel NADPH thioredoxin reductase, localized in the chloroplast, which deficiency causes hypersensitivity to abiotic stress in *Arabidopsis thaliana*. The Journal of Biological Chemistry **279**, 43821-43827.

Stöcker S, Maurer M, Ruppert T, Dick TP. 2017. A role for 2-Cys peroxiredoxins in facilitating cytosolic protein thiol oxidation. Nature Chemical Biology **14**, 148-155.

Vaseghi MJ, Chibani K, Telman W, Liebthal MF, Gerken M, Schnitzer H, Mueller SM, Dietz KJ. 2018. The chloroplast 2-cysteine peroxiredoxin functions as thioredoxin oxidase in redox regulation of chloroplast metabolism. eLife **7,** e38194 DOI: 10.7554/eLife.38194.

Vieira Dos Santos C, Rey P. 2006. Plant thioredoxins are key actors in oxidative stress response. Trends in Plant Science **11**, 329-334.

Wood ZA, Poole LB, Karplus PA. 2003. Peroxiredoxin evolution and the regulation of hydrogen peroxide signaling. Science **300**, 650-653.

Xia XJ, Fang PP, Guo X, Qian XJ, Zhou J, Shi K, Zhou YH, Yu JQ. 2018. Brassinosteroid-mediated apoplastic H_2O_2-glutaredoxin 12/14 cascade regulates antioxidant capacity in response to chilling in tomato. Plant Cell & Environment **41**, 1052-1064.

Yang Y, Cai W, Wang J, Pan W, Liu L, Wang M, Zhang M.2018 Crystal structure of Arabidopsis thaliana peroxiredoxin A C119S mutant. Acta Crystallographica **F74**, 625-631.

Yoshida K, Hara A, Sugiura K, Fukaya Y, Hisabori T. 2018. Thioredoxin-like2/2-Cys peroxiredoxin redox cascade supports oxidative thiol modulation in chloroplasts. Proceedings of the National Academy of Sciences of the United States of America **115**, E8296-E8304.

Yoshida K, Matsuoka Y, Hara S, Konno H, Hisabori T. 2014. Distinct redox behaviors of chloroplast thiol enzymes and their relationships with photosynthetic electron transport in Arabidopsis thaliana. Plant & Cell Physiology **55**, 1415-1425.

Legends to figures

Figure 1. 2-CysPRX monomer and dimer distribution in Arabidopsis, barley and potato leaves.

A and **B**. Western blot analysis of 2-CysPRX abundance in leaves from 6-week Arabidopsis old plants prepared and migrated in reducing (**A**) or non-reducing conditions (**B**) (10 µg per lane).

WT, wild type Arabidopsis Col-0 plants ; *a* and *b*, *2-cysprxa* and *2-cysprxb* homozygous plants from the GK_295C05 and SALK_017213 lines, respectively; *ab*, *2-cysprxa 2-cysprxb* double mutant generated from the crossing of single mutant lines; *ntrc*, SALK_096776 homozygous plants; *srx*, SALK_015324 homozygous plants.

C and **D**. Western blot analysis of 2-CysPRX abundance in leaves from 6-week old Arabidopsis plants and 3-week-old barley and potato plants prepared and migrated in reducing (**C**) or non-reducing conditions (**D**) (12 µg per lane).

At, Arabidopsis WT Col-0; *ntrc*, SALK_096776 homozygous Arabidopsis mutant; Hv, barley WT cv. "Express"; St, potato WT cv. "Désirée". CB, Coomassie-blue stained gel in the 50-kDa range as a loading control; WB, Western blot.

Figure 2. Thiol content in 2-CysPRXs from Arabidopsis, barley and potato leaves.

A. Western blot analysis of 2-CysPRX abundance in leaves from 6-week Arabidopsis old plants prepared in non-reducing conditions, incubated with mPEG-maleimide-2000 and migrated in non-reducing conditions (50 µg per lane).

B. Western blot analysis of 2-CysPRX abundance in leaves from 6-week Arabidopsis old plants prepared in reducing or non-reducing conditions, incubated or not in the presence of mPEG-maleimide-2000 and migrated in the presence of reductant (12 µg per lane).

WT, wild type Col-0 ; *2-cysprxa* and *2-cysprxb*, homozygous plants from the GK_295C05 and SALK_017213 lines, respectively; *2-cysprxa 2-cysprxb*, double mutant generated from the crossing of the single mutant lines; *ntrc*, SALK_096776 homozygous plants; *srx*, SALK_015324 homozygous plants.

C. Western blot analysis of 2-CysPRX abundance in leaves from 6-week old WT Arabidopsis plants prepared in reducing (either TCEP or β-mercaptoethanol) or non-reducing conditions, incubated or not in the presence of mPEG-maleimide-2000 and migrated in the presence of reductant (12 µg per lane).

D. Western blot analysis of 2-CysPRX abundance in leaves from 6-week old Arabidopsis plants and 3-week-old barley and potato plants prepared in reducing (50 mM TCEP) or non-reducing conditions, incubated or not in the presence of mPEG-maleimide-2000 and migrated in the presence of reductant (12 µg per lane). At, Arabidopsis WT Col-0; Hv, barley WT cv. "Express"; St, potato WT cv. "Désirée".

Asterisks and arrows on the right indicate additional bands.

Figure 3. Redox status of 2-CysPRXs in Arabidopsis leaves as a function of light cycle.

A and **B**. Western blot analysis of 2-CysPRX abundance and hyperoxidation level in leaves from 6-week old Arabidopsis WT plants as a function of light cycle. Proteins were prepared and migrated in the presence of reductant (**A**) or not (**B**). (10 and 12 µg per lane in **A** and **B**, respectively).

C. Relative abundance of 2-CysPRX abundance detected in reducing and non-reducing conditions following the light-dark transition compared to the dark-light transition. Band intensities from L1 and D2 light time points were quantified as described in Material and Methods. Data are means of values ± SD originating from three and five independent experiments in reducing and non-reducing conditions, respectively. **, values significantly different with $P < 0.01$ (*t*-test).

D. Western blot analysis of 2-CysPRX abundance in leaves from 6-week old *ntrc* and *srx* plants as a function of light cycle. Proteins were prepared and migrated in the absence of reductant (12 µg per lane).

E. Western blot analysis of 2-CysPRX abundance following alkylation in leaves from 6-week old WT Arabidopsis plants as a function of light cycle. Proteins were prepared in non-reducing conditions, incubated with mPEG-maleimide-2000 and migrated in the presence of reductant (12 µg per lane). The arrow on the right indicates additional bands.

Light time points: D1 and L1, 45 min before and after the dark-light transition, respectively; L2, middle of the 8-h light period; L3 and D2, 45 min before and after the light-dark transition, respectively. CB, Coomassie-blue stained gels in the 50-kDa (**A-B, D**) or 25-kDa (**E**) ranges as loading controls; WB, Western blot.

Figure 4. Redox status of 2-CysPRXs in barley and potato leaves as a function of light cycle.

A and **B**. Western blot analysis of 2-CysPRX abundance and hyperoxidation level in leaves from 3-week old barley (**A**) and potato (**B**) WT plants as a function of light cycle. Proteins were prepared and migrated in the presence of reductant (10 µg per lane).

C and **D**. Western blot analysis of 2-CysPRX abundance in leaves from 3-week old barley (**C**) and potato (**D**) WT plants as a function of light cycle. Proteins were prepared and migrated in the absence of reductant (12 µg per lane).

E and **F**. Western blot analysis of 2-CysPRX abundance following alkylation in leaves from 3-week old barley (**E**) and potato (**F**) WT plants as a function of the light time point. Proteins were prepared in non-reducing conditions, incubated with mPEG-maleimide-2000 and migrated in reducing conditions (12 µg per lane). The arrow on the right indicates additional bands.

Light time points: D1 and L1, 45 min before and after the dark-light transition, respectively; L2, middle of the 8-h and 12-h light periods for barley and potato, respectively; L3 and D2, 45 min before and after the light-dark transition, respectively.

CB, Coomassie Blue-stained gels in the 50-kDa (**A**-**D**) or 25-kDa (**E**-**F**) ranges as loading controls; WB, Western blot.

Figure 5. Redox status of 2-CysPRXs in potato plants modified for *CDSP32* expression.

A. Western blot analysis of 2-CysPRX abundance and hyperoxidation level in leaves from 3-week old potato plants. Proteins were prepared and migrated in the presence of reductant (10 µg per lane).

B. Western blot analysis of 2-CysPRX abundance in leaves from 3-week old potato plants. Proteins were prepared and migrated in the absence of reductant (12 µg per lane).

C. Western blot analysis of 2-CysPRX abundance following alkylation in leaves from 3-week old potato plants. Proteins were prepared in non-reducing conditions, incubated with mPEG-maleimide-2000 and migrated in reducing conditions (12 µg per lane). The arrow on the right indicates additional bands.

WT, wild type cv. "Désirée"; CS, line co-suppressed for *CDSP32* expression; OE, line over-expressing WT *CDSP32*; OE-M1 and OE-M2, two independent lines over-expressing a *CDSP32* gene coding for a mutated active site form. Leaf samples were collected at the L3 light time point (45 min before the light-dark transition). CB, Coomassie Blue-stained gels in the 50-kDa (**A**-**B**) or 25-kDa (**C**) ranges as loading controls; WB, Western blot.

Figure 6. Hyperoxidation of plant 2-CysPRXs.

A. Western blot analysis of 2-CysPRX abundance and hyperoxidation level in Arabidopsis leaves as a function of developmental stage in 6-week old plants using sera raised against At2-CysPRX and hyperoxidized 2-CysPRX (10 µg per lane).

B. Relative abundances compared to WT of total and hyperoxidized 2-CysPRX in leaves from 6-week old Arabidopsis *2-cysprxa* and *2-cysprxb* plants. Band intensity was quantified as described in Material and Methods. Data are means of values ± SD originating from three independent plants. *, ** and ***, values significantly different with $P < 0.05$, $P < 0.01$ and $P < 0.001$, respectively (*t*-test).

C. Western blot analysis of 2-CysPRX abundance and hyperoxidation level in leaves from 6-week old Arabidopsis plants and 3-week-old barley and potato plants (10 µg per lane). Arabidopsis and barley leaves were collected 45 min following the dark-light transition and potato leaves 45 min before the light-dark transition,

WT and At, wild type Arabidopsis Col-0; *2-cysprxa* and *2-cysprxb*, homozygous plants from the GK_295C05 and SALK_017213 lines, respectively. Y, young leaf; A, adult leaf; O, old leaf**.** Hv, barley WT cv. "Express"; St, potato WT cv. "Désirée". CB, Coomassie-blue stained gel in the 50-kDa range as a loading control; WB, Western blot.

Figure 7. **Sequence and structural comparisons of plant 2-Cys peroxiredoxins.**

A. Sequence aligment of Arabidopsis, potato and barley 2-CysPRXs. NCBI references for Arabidopsis 2-Cys PRXs A and B: NP_187769.1 and NP_568166.1, respectively. NCBI reference for potato: XP_006339159.1. GenBank reference for barley: BAJ98505.1. The motifs A and B, involved in hyperoxidation resistance (Bolduc *et al.*, 2018), are highlighted in blue and yellow, respectively. The GGLG and YF motifs that are considered as a signature of sensitivity to hyperoxidation are highlighted in gray. The two catalytic Cys are highlighted in purple. Residues highlighted in red and green are specific to Hv2-CysPRX and to At2-CysPRXB, respectively, within motifs A and B. Two-by-two sequence alignments were made using At2-CysPRXA as a reference.

B. and C. Structural comparison of At2-CysPRXA and Hv2-CysPRX. Ribbon representation of At2-CysPRXA C119A (PDB code 5ZTE monomer C) and Hv2-CysPRX (3D structural model) showing motifs A, B, GGLG and YF and position of the two different residues within motif A highlighted in red in Fig. 7A (left). Surface representation displaying atoms color-coded according to the surface potential from red (negative) to blue (positive)

(right). All images were created using PyMOL.

Figure 8. Model for the hierarchy of the resistance of plant 2-CysPRXs to hyperoxidation. The model is adapted from Bolduc *et al.*, (2018). Based on the presence or not of GGLG/YF, A and B motifs, the bacterial AhpC and the human HsPRX2 are the most resistant and sensitive, respectively. Human HsPRX3 like plant 2-Cys-PRXs displays motifs A and B. The proposed graded resistance of plant 2-CysPRXs is based on the sequence features of At2-CysPRXB and Hv2-CysPRx within or very close to motifs A and B.

Supplementary data

Figure S1: Time points for collecting leaf samples during the light cycle. D1 and L1 correspond to 45 min before and after the dark-light transition, respectively, L2 to the middle of the light period, and L3 and D2 to 45 min before and after the light-dark transition. The photoperiod length is 8 h for Arabidopsis and barley, and 12 h for potato.

Figure S2. **Thiol content in 2-CysPRX in Arabidopsis *ntrc* leaves as a function of light cycle.**

Western blot analysis of 2-CysPRX abundance following alkylation in leaves from 6-week old Arabidopsis *ntrc* plants as a function of light cycle. Proteins were prepared in non-reducing conditions, incubated in the presence of mPEG-maleimide-2000 and migrated in the presence of reductant (12 µg per lane). The arrow on the right indicates additional bands.
Light time points: D1 and L1, 45 min before and after the dark-light transition, respectively; L3 and D2, 45 min before and after the light-dark transition, respectively. CB, Coomassie-blue stained gel in the 25-kDa range as a loading control; WB, Western blot.

Figure S3. Structural comparison of At2-CysPRXA (A) and At2-CysPRXB (B). Ribbon (left) and ball (right) representation of At2-CysPRXA C119A (PDB code 5ZTE dimer BC) and At2-CysPRXB (3D structural model) showing motifs A and B and the position of the different residue in green preceding the motif B. All images were created using PyMOL.

Figure S4: **Sequence alignment of plant 2-Cys peroxiredoxins.**

NCBI or Genbank references: *Arabidopsis thaliana* 2-Cys PRXs A and B, NP_187769.1 and NP_568166.1, respectively; *Camelina sativa* (Cs), XP_010464879.1; *Raphanus sativus* (Rs), XP_018493095.1; *Papaver somniferum* (Ps), XP_026426631.1; *Prunus persica* (Pp), XP_007202444.1; *Glycine max* (Gm), NP_001341836.1; *Spinacia oleracea* (St), XP_021867340.1; *Solanum tuberosum* (St): XP_006339159.1; *Helianthus annuus* (Ha), XP_021984163.1; *Hordeum vulgare* (Hv), BAJ98505.1; *Triticum aestivum* (Ta), SPT18356.1; *Zea mays* (Zm), NP_001137046.1. The motifs A and B, involved in hyperoxidation resistance of 2-Cys peroxiredoxins (Bolduc *et al.*, 2018), are highlighted in blue and yellow, respectively. The GGLG and YF motifs considered as a signature of sensitivity to hyperoxidation are highlighted in gray. The two catalytic Cys are highlighted in purple. Black bars indicate sequence divergence within motifs A and B.

Fig. 1

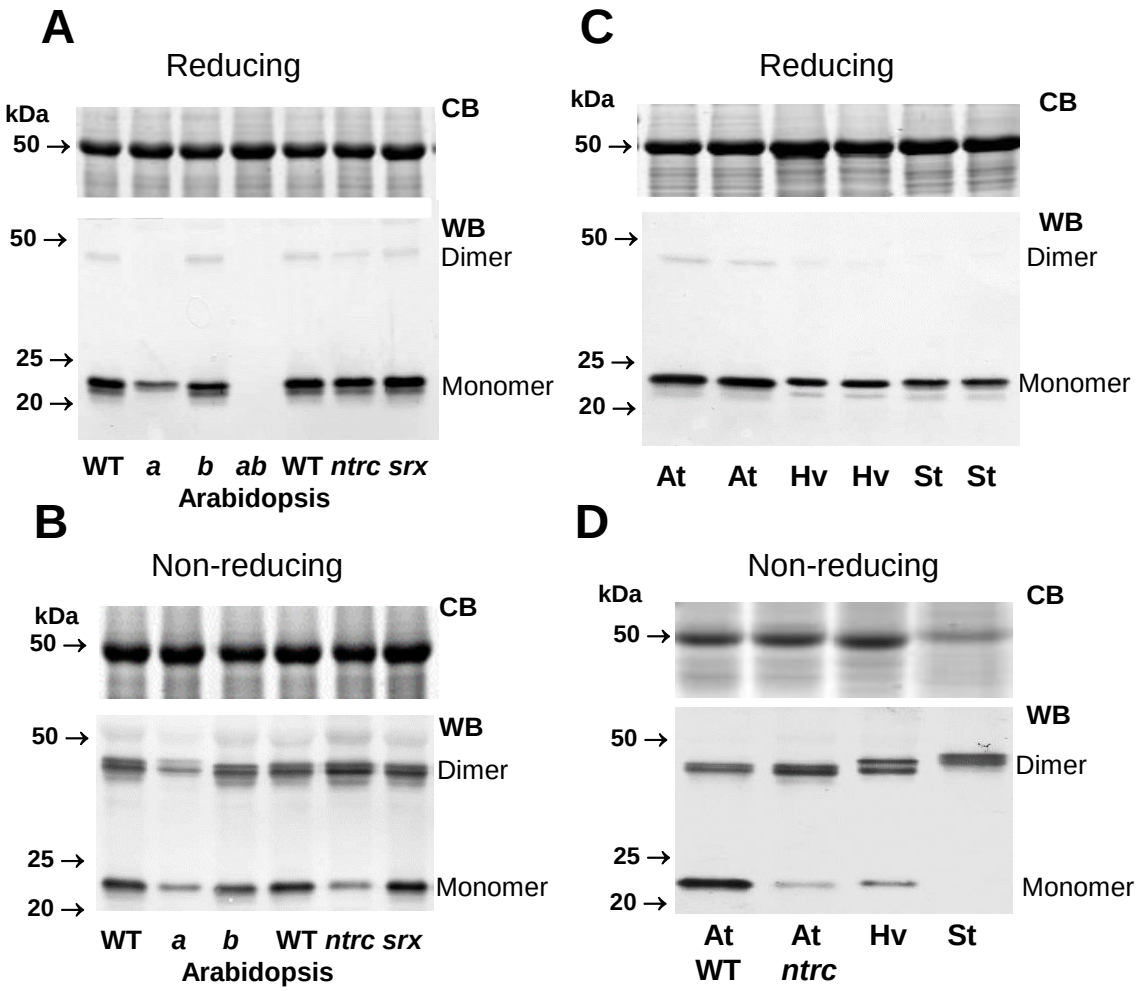
A
Reducing
kDa
50 →
CB
50 →
WB
Dimer
25 →
20 →
Monomer
WT a b ab WT ntrc srx
Arabidopsis
C
Reducing
kDa
50 →
CB
50 →
WB
Dimer
25 →
20 →
Monomer
At At Hv Hv St St
B
Non-reducing
kDa
50 →
CB
50 →
WB
Dimer
25 →
20 →
Monomer
WT a b WT ntrc srx
Arabidopsis
D
Non-reducing
kDa
50 →
CB
50 →
WB
Dimer
25 →
20 →
Monomer
At At Hv St
WT ntrc

Fig.2

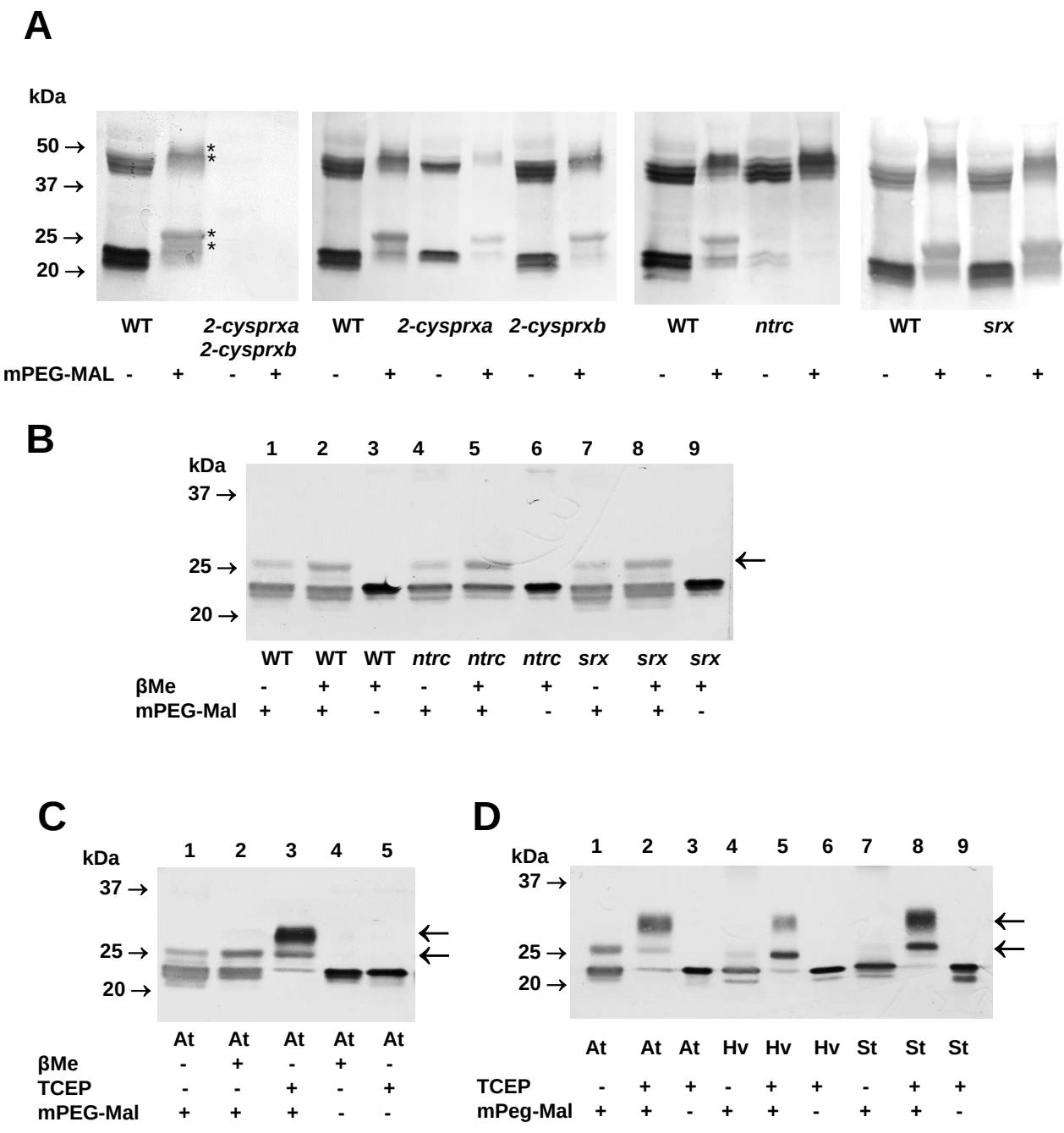
A
kDa
50 →
37 →
25 →
20 →
WT
2-cysprxa 2-cysprxb
WT
2-cysprxa
2-cysprxb
WT
ntrc
WT
srx
mPEG-MAL - + - + - + - + - + - + - + - + - + - +
B
1 2 3 4 5 6 7 8 9
kDa
37 →
25 →
20 →
WT WT WT ntrc ntrc ntrc srx srx srx
βMe - + + - + + - + +
mPEG-Mal + + - + + - + + -
C
kDa
1 2 3 4 5
37 →
25 →
20 →
At At At At At
βMe - + - + -
TCEP - - + - +
mPEG-Mal + + + - -
D
kDa
1 2 3 4 5 6 7 8 9
37 →
25 →
20 →
At At At Hv Hv Hv St St St
TCEP - + + - + + - + +
mPeg-Mal + + - + + - + + -

Fig. 3

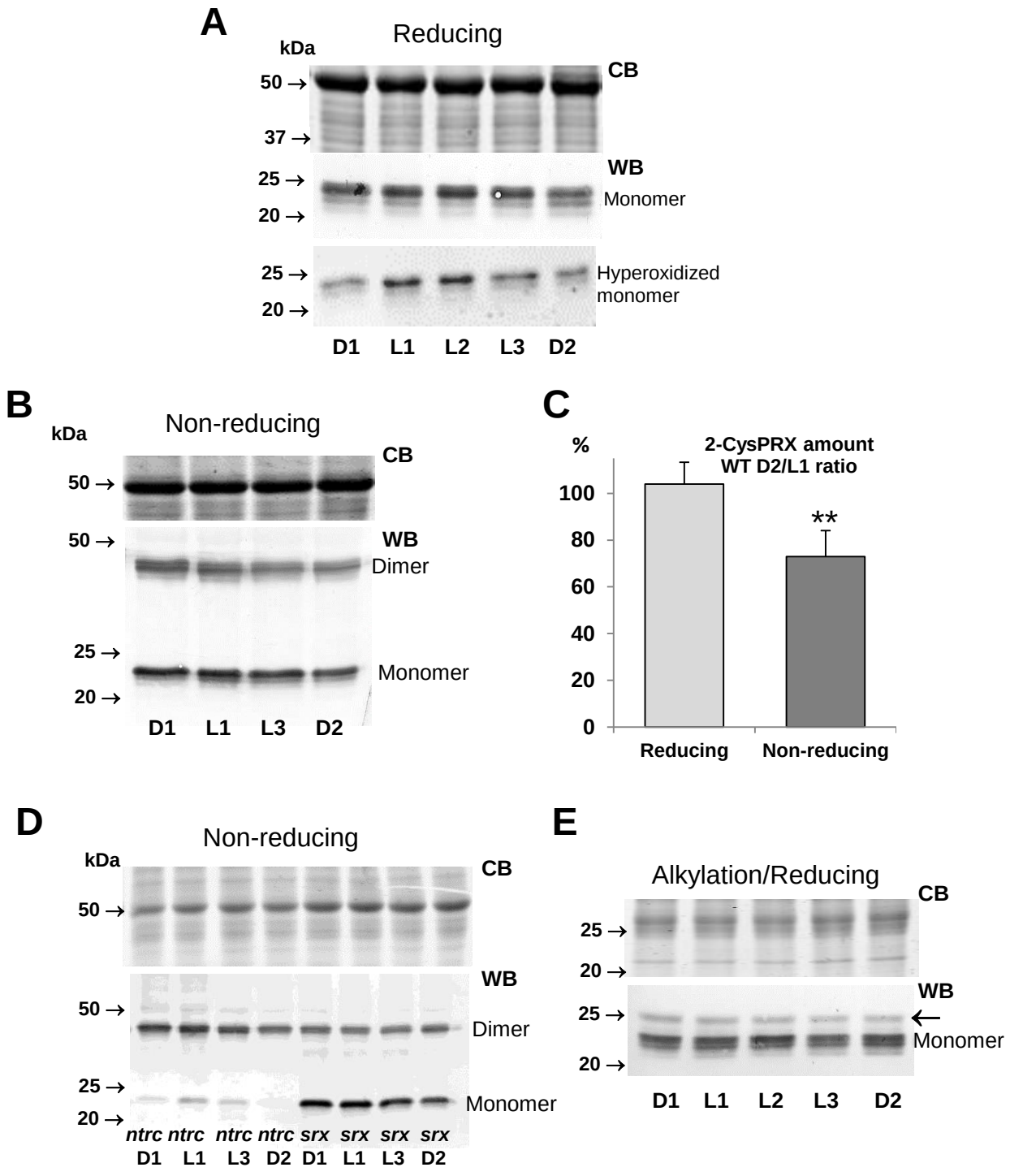
A
Reducing
kDa
50 →
37 →
CB
25 →
20 →
WB
Monomer
25 →
20 →
Hyperoxidized monomer
D1 L1 L2 L3 D2
B
Non-reducing
kDa
50 →
CB
50 →
WB
Dimer
25 →
20 →
Monomer
D1 L1 L3 D2
C
2-CysPRX amount
WT D2/L1 ratio
%
100
80
60
40
20
0
**
Reducing
Non-reducing
D
Non-reducing
kDa
50 →
CB
WB
50 →
Dimer
25 →
20 →
Monomer
ntrc ntrc ntrc ntrc srx srx srx srx
D1 L1 L3 D2 D1 L1 L3 D2
E
Alkylation/Reducing
25 →
20 →
CB
WB
25 →
Monomer
20 →
D1 L1 L2 L3 D2

Fig. 4

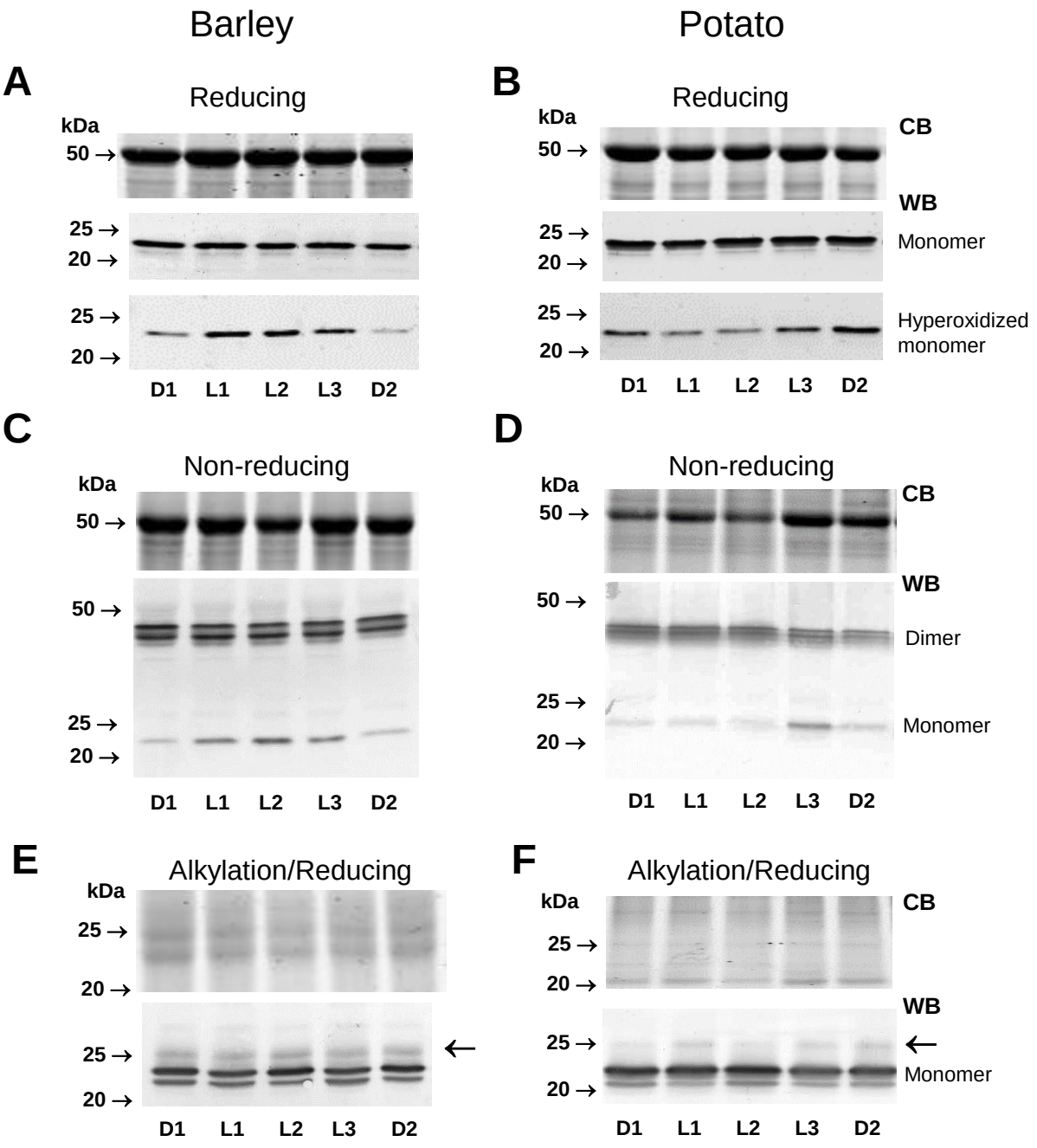
Barley
Potato
A
Reducing
kDa
50 →
25 →
20 →
25 →
20 →
D1 L1 L2 L3 D2
B
Reducing
kDa
50 →
CB
WB
25 →
20 →
Monomer
25 →
20 →
Hyperoxidized monomer
D1 L1 L2 L3 D2
C
Non-reducing
kDa
50 →
50 →
25 →
20 →
D1 L1 L2 L3 D2
D
Non-reducing
kDa
50 →
CB
WB
50 →
Dimer
25 →
20 →
Monomer
D1 L1 L2 L3 D2
E
Alkylation/Reducing
kDa
25 →
20 →
25 →
20 →
←
D1 L1 L2 L3 D2
F
Alkylation/Reducing
kDa
25 →
20 →
CB
WB
25 →
20 →
←
Monomer
D1 L1 L2 L3 D2

Fig. 5

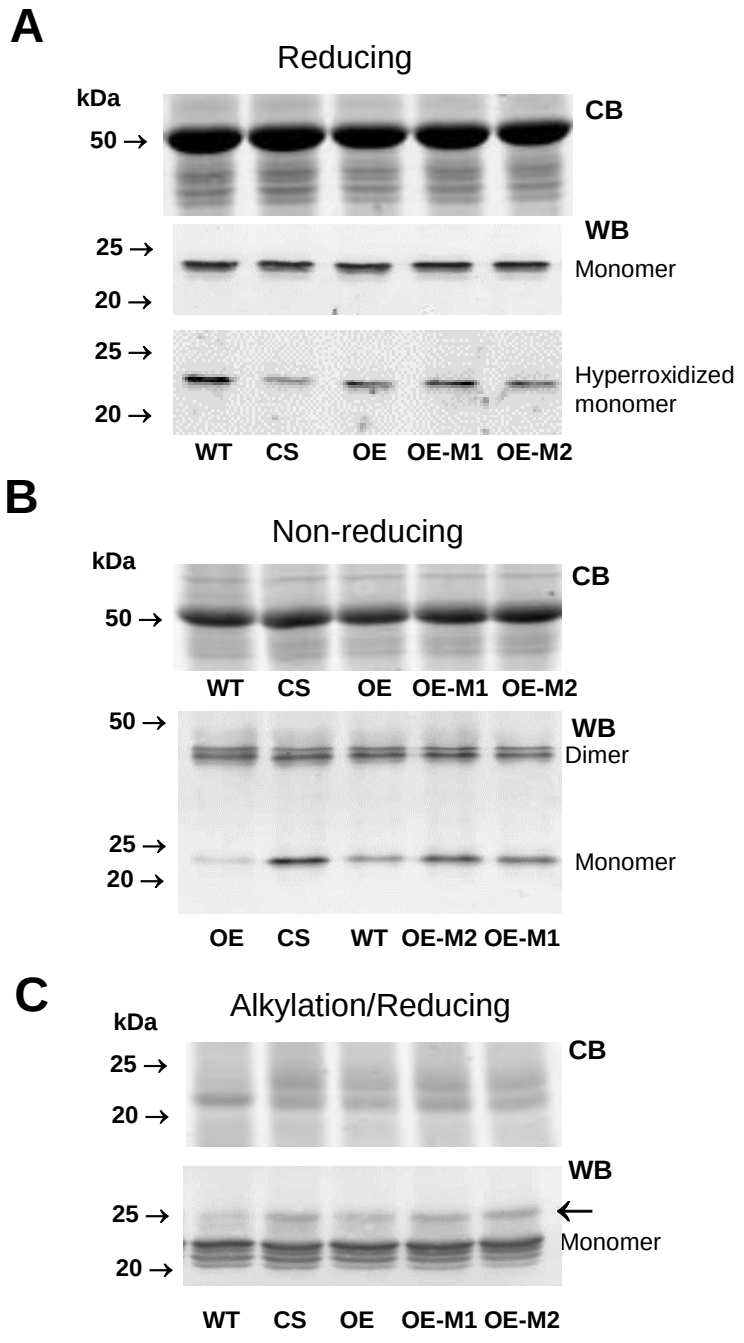
A
Reducing
kDa
50 →
CB
WB
25 →
20 →
Monomer
25 →
20 →
Hyperroxidized monomer
WT CS OE OE-M1 OE-M2
B
Non-reducing
kDa
50 →
CB
WT CS OE OE-M1 OE-M2
50 →
WB
Dimer
25 →
20 →
Monomer
OE CS WT OE-M2 OE-M1
C
Alkylation/Reducing
kDa
25 →
20 →
CB
WB
25 →
20 →
Monomer
WT CS OE OE-M1 OE-M2

Fig.6

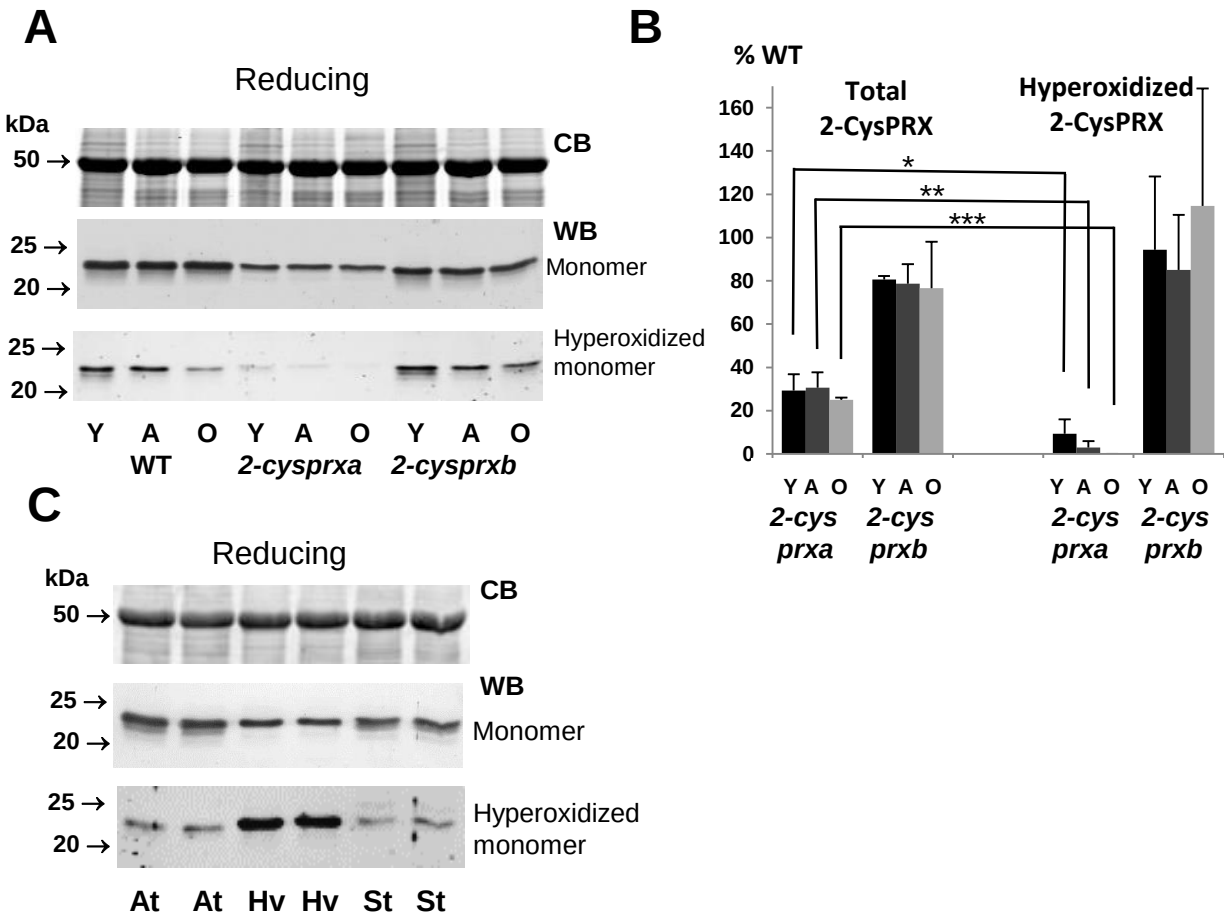
A
Reducing
kDa
50 →
CB
25 →
20 →
WB
Monomer
25 →
20 →
Hyperoxidized
monomer
Y A O Y A O Y A O
WT
2-cysprxa
2-cysprxb
B
% WT
Total
2-CysPRX
Hyperoxidized
2-CysPRX
160
140
120
100
80
60
40
20
0
*
**
***
Y A O Y A O Y A O Y A O
2-cys prxa
2-cys prxb
2-cys prxa
2-cys prxb
C
Reducing
kDa
50 →
CB
25 →
20 →
WB
Monomer
25 →
20 →
Hyperoxidized
monomer
At At Hv Hv St St

Fig. 7

A

```
At2-CysPRXA   67  -AQADDLPLVGNKAPDFEAEAVFDQEFIKVKLSDYIGKKYVILFFYPLDFTFVCPTEITA
At2-CysPRXB   74  -AQADDLPLVGNKAPDFEAEAVFDQEFIKVKLSEYIGKKYVILFFYPLDFTFVCPTEITA
St2-CysPRX    69  --ASSELPLVGNQAPDFEAEAVFDQEFIKVKLSEYIGKKYVILFFYPLDFTFVCPTEITA
Hv2-CysPRX    62  AAAEYDLPLVGNKAPDFAAEAVFDQEFINVKLSDYIGKKYVILFFYPLDFTFVCPTEITA
                      :******:**** **********:****:**************************

At2-CysPRXA  126  FSDRHSEFEKLNTEVLGVSVDSVFSHLAWVQTDRKSGGLGDLNYPLISDVTKSISKSFGV
At2-CysPRXB  133  FSDRYEEFEKLNTEVLGVSVDSVFSHLAWVQTDRKSGGLGDLNYPLVSDITKSISKSFGV
St2-CysPRX   127  FSDRYEEFEKVNTEVLGVSVDSVFSHLAWVQTERKSGGLGDLNYPLISDVTKSISKSYNV
Hv2-CysPRX   122  FSDRHEEFEKINTEILGVSVDSVFSHLAWVQTERKSGGLGDLKYPLVSDVTKSISKSFGV
                  ****:.****:***:*****************:*********:***:**:*******:.*
                        Motif A:D-X8-N/G-X"10"-H-X"27"-S/G     Motif B:T-X3-S

At2-CysPRXA  186  LIHDQGIALRGLFIIDKEGVIQHSTINNLGIGRSVDETMRTLQALQYIQENPDEVCPAGW
At2-CysPRXB  193  LIPDQGIALRGLFIIDKEGVIQHSTINNLGIGRSVDETMRTLQALQYVQENPDEVCPAGW
St2-CysPRX   187  LIPDQGIALRGLFIIDKEGVIQHSTINNLGIGRSVDETLRTLQALQYVQENPDEVCPAGW
Hv2-CysPRX   182  LIPDQGIALRGLFIIDKEGVIQHSTINNLGIGRSVDETLRTLQALQYVQENPDEVCPAGW
                  ** ***********************************:********:************

                                                  Overlap   Identity   Similarity
At2-CysPRXA  246  KPGEKSMKPDPKLSKEYFSAI  266
At2-CysPRXB  253  KPGEKSMKPDPKLSKEYFSAI  273       200 AA     96.5%       99.0%
St2-CysPRX   247  KPGEKSMKPDPKGSKEYFASI  267       198 AA     91.4%       98.5%
Hv2-CysPRX   242  KPGEKSMKPDPKGSKEYFAAI  262       200 AA     92.0%       96.5%
                  ************ ******::*
```

B

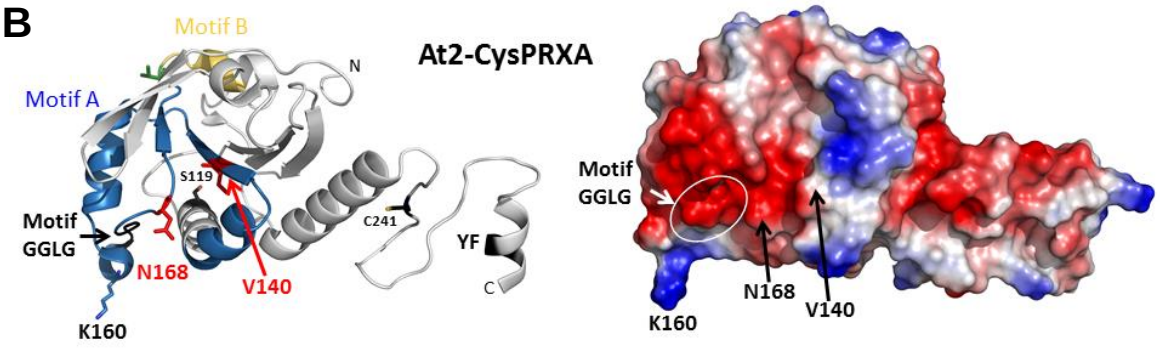

C

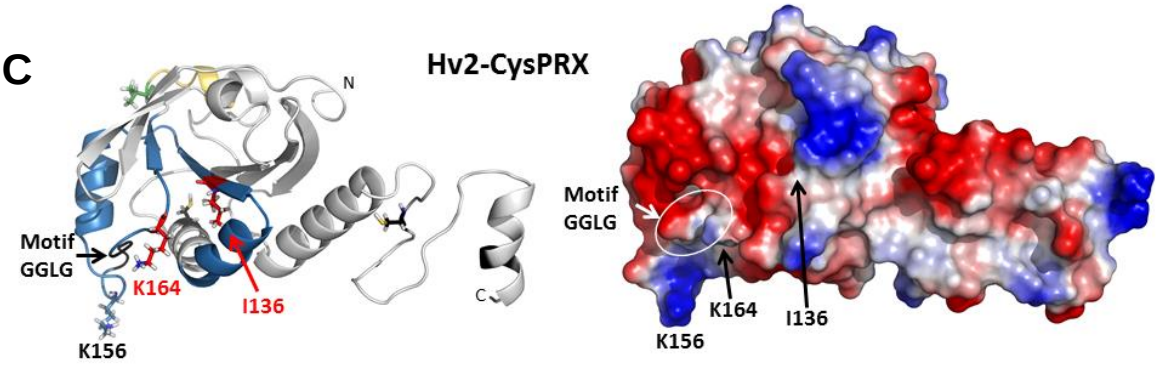

Fig. 8

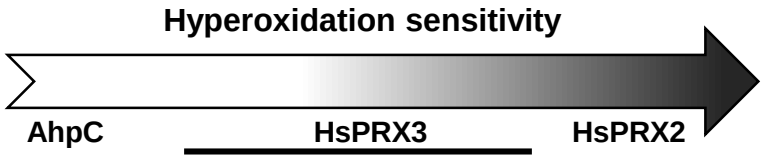

	AhpC	HsPRX3			HsPRX2
		AtPRXB	AtPRXA	HvPRX StPRX	
YF/GGLG	–	+	+	+	+
Motif A	+	+	+	+ (I136-X_{27}-K)	–
Motif B	+	+ (I182-Motif B)	+	+	+

Variability in the redox status of plant 2-Cys peroxiredoxins in relation to species and light cycle

Delphine Cerveau[1], Patricia Henri[1], Laurence Blanchard[2] and Pascal Rey[1, *]

[1] Aix Marseille Univ, CEA, CNRS, BIAM, Plant Protective Proteins Team, Saint Paul-Lez-Durance, France F-13108

[2] Aix Marseille Univ, CEA, CNRS, BIAM, Molecular and Environmental Microbiology Team, Saint Paul-Lez-Durance, France F-13108

Mail adresses :

Delphine Cerveau: delphine.cerveau@yahoo.com

Patricia Henri: patricia.henri@cea.fr

Laurence Blanchard: laurence.blanchard@cea.fr

Pascal Rey: pascal.rey@cea.fr

*Corresponding author: Pascal Rey

Plant Protective Proteins Team, Bâtiment 158, BIAM, CEA Cadarache, Saint-Paul-lez-Durance, F-13108, France

Phone: ++33 442254776

E-mail: pascal.rey@cea.fr

Date of submission: April 9, 2019

Number of tables: 0

Number of figures: 8 (seven in black and white and one in color)

Word count; *ca* 6035

Supplementary data: Four figures

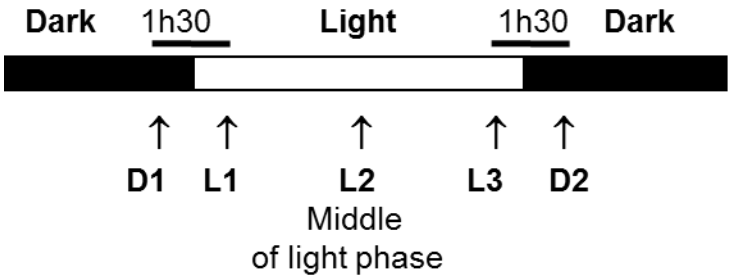

Figure S1: Time points for collecting leaf samples during the light cycle. D1 and L1 correspond to 45 min before and after the dark-light transition, respectively, L2 to the middle of the light period, and L3 and D2 to 45 min before and after the light-dark transition. The photoperiod length is 8 h for Arabidopsis and barley, and 12 h for potato.

Fig. S2

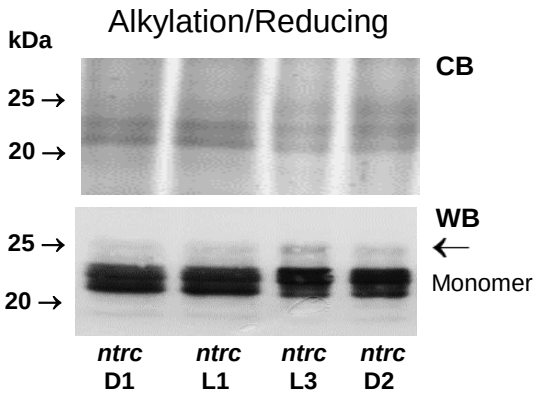

Figure S2. **Thiol content in 2-CysPRX in Arabidopsis *ntrc* leaves as a function of light cycle.**
Western blot analysis of 2-CysPRX abundance following alkylation in leaves from 6-week old Arabidopsis *ntrc* plants as a function of light cycle. Proteins were prepared in non-reducing conditions, incubated in the presence of mPEG-maleimide-2000 and migrated in the presence of reductant (12 µg per lane). The arrow on the right indicates additional bands. Light time points: D1 and L1, 45 min before and after the dark-light transition, respectively; L3 and D2, 45 min before and after the light-dark transition, respectively. CB, Coomassie-blue stained gel in the 25-kDa range as a loading control; WB, Western blot.

Fig. S3

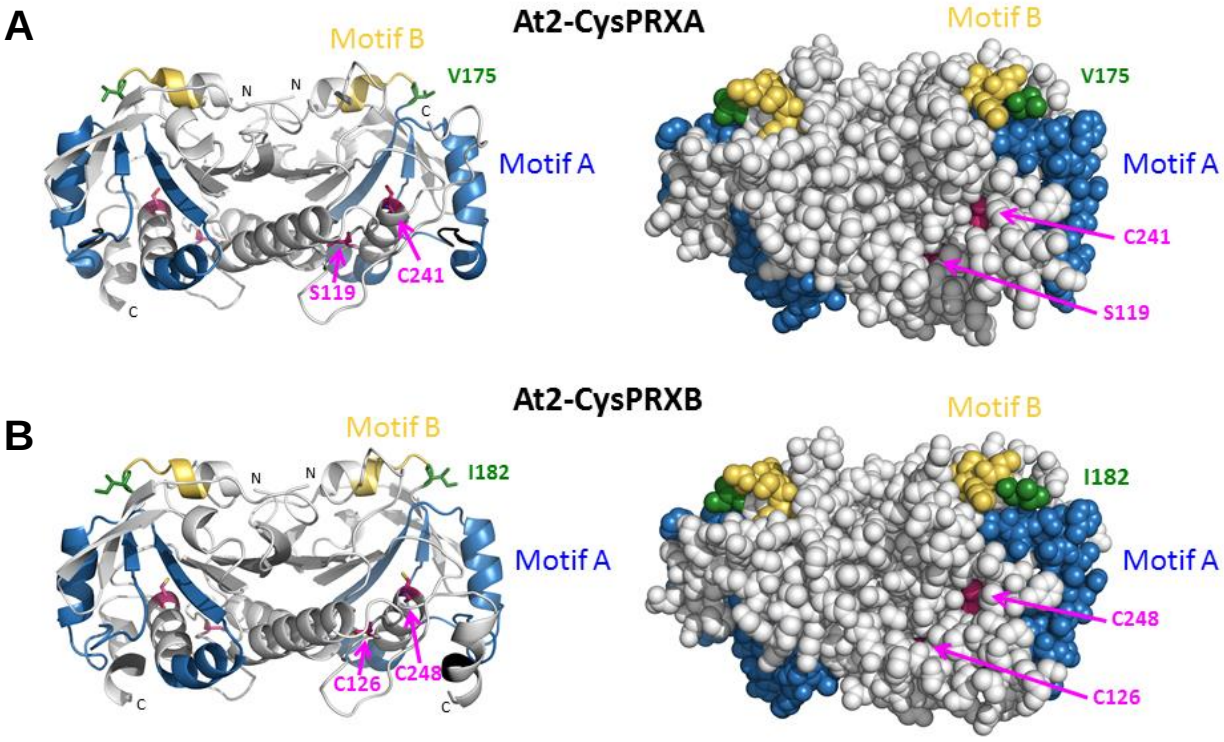

Figure S3. Structural comparison of At2-CysPRXA (A) and At2-CysPRXB (B). Ribbon (left) and ball (right) representation of At2-CysPRXA C119A (PDB code 5ZTE dimer BC) and At2-CysPRXB (3D structural model) showing motifs A and B and the position of the different residue in green preceding the motif B. All images were created using PyMOL.


At2-CysPRXA 1 ---MASVASSTTLISSPSSRVFPAKSSLSSPSVSFLRTLSSP-SASASLRSGFARRSSLSS---TSRRSFAVKAQADDLPLVGNKAPDFEAEAVFDQEF
At2-CysPRXB 1 MSMASIASSSSTTLLSSSRVLLPSKSSLLSPTVSFPRIIPSSSASSSSLCSGFSSLGSLTTNRSASRRNFAVKAQADDLPLVGNKAPDFEAEAVFDQEF
Cs2-CysPRX 1 ---MASVASSTTLISSPSSRVFPVKSSLSSPSVSFLRTLSSPSASAVALRSGFARRSSLTS---TSRRSFAVKAQADELPLVGNKAPDFEAEAVFDQEF
Rs2-CysPRX 1 ---MASVASSTTLISS-STRALPAKSPLPSPSISFLPTLSSPLRSGFSQRS---SLTSIRS---TSRRSFAVKAQTDDLPLVGNKAPDFEAEAVFDQEF
Ps2-CysPRX 1 ----MACSASSTVISSNPSSIKFPKPMASLTSSLPFSQTLNVPKSFNGLRNSFQSRASRSISTNQSKRSLVVKASAGELPLVGNKAPDFEAEAVFDQEF
Pp2-CysPRX 1 ---MAASTALISSTPSRAFSSKSTPLVASSSISKPISQTLTFPKSFNGLRLPRVAHSVSLSRGAHSRRSFLVKASVDELPLVGNVAPDFEAEAVFDQEF
Gm2-CysPRX 1 --------MACSATSASLFSANPTPLFSPKSS-------LSLPNNSLHLNPLPTRPSLSLTRPSHTRRSFVVKASSSELPLVGNTAPDFEAEAVFDQEF
So2-CysPRX 1 ---MACAASSSAILSPNPRVFAAKSHAPMAAASVSSLPKPFSQTLTLSSNFNGVRKSFQSPRRAQSSRSSFVVRASAELPLVGNVAPDFEAEAVFDQEF
St2-CysPRX 1 ------MACSASSSTALLSSTSRASISPKSHISQSISVPSAFNGLRNCKPFVSRVARSISTRVAQSERRRFAVCASSELPLVGNQAPDFEAEAVFDQEF
Ha2-CysPRX 1 ---MASLSASAALLSSNPRYISPKSSNLSQTLSFLGSSSVNFRSKSLRS----------ALAVRPSASRCNGSLIKAALPLVGNKAPDFEAEAVFDQEF
Hv2-CysPRX 1 -----------MACAISASTVSTAAALVASPKTSGAPQCLSFPRAFGGAAARPARLAAAGSRTARARSFVARAAAEYDLPLVGNKAPDFAAEAVFDQEF
Ta2-CysPRX 1 -----------MACAFSASTVSTAAALVASPKPAGVPQCLSFP----RAAARPSRLAAAGSRTARARSFVARAAAEYDLPLVGNKAPDFAAEAVFDQEF
Zm2-CysPRX 1 -----------MACSFAAATVVSSAPTPAARPLAVAPQSVSVSRSAVATAARPLRLVAS--RSARATRLVARAGGVDDLPLVGNKAPDFEAEAVFDQEF
At2-CysPRXA 93 IKVKLSDYIGKKYVILFFYPLDFTFVCPTEITAFSDRHSEFEKLNTEVLGVSVDSVFSHLAWVQTDRKSGGLGDLNYPLISDVTKSISKSFGVLIHDQG
At2-CysPRXB 102 IKVKLSEYIGKKYVILFFYPLDFTFVCPTEITAFSDRYEEFEKLNTEVLGVSVDSVFSHLAWVQTDRKSGGLGDLNYPLVSDITKSISKSFGVLIPDQG
Cs2-CysPRX 94 IKVKLSEYIGKKYVILFFYPLDFTFVCPTEITAFSDRYSEFEKLNTEVLGVSVDSVFSHLAWVQTDRKSGGLGDLNYPLVSDVTKSIAKSFGVLIHDQG
Rs2-CysPRX 90 IKVKLSEYIGKKYVILFFYPLDFTFVCPTEITAFSDRYAEFEKLNTEVLGVSVDSVFSHLAWVQTDRKSGGLGDLNYPLVSDVTKSISKSFGVLIPDQG
Ps2-CysPRX 96 IKVKLSDYIGKKYVILFFYPLDFTFVCPTEITAFSDRHAEFEKLDTEILGVSVDSVFSHLAWVQTDRKSGGLGDLNYPLVSDVTKSISKAYDVLIADQG
Pp2-CysPRX 97 IKVKLSEYIGKKYVILFFYPLDFTFVCPTEITAFSDRHAEFEELNTEILGVSVDSVFSHLAWVQTDRKSGGLGDLNYPLISDVTKSISKSYDVLIPDQG
Gm2-CysPRX 85 INVKLSDYIGKKYVVLFFYPLDFTFVCPTEITAFSDRHAEFEALNTEILGVSVDSVFSHLAWIQTDRKSGGLGDLNYPLISDVTKSISKSYGVLIPDQG
So2-CysPRX 97 INVKLSDYRGKKYVILFFYPLDFTFVCPTEITAFSDRHGEFEKLNTEILGVSVDSVFSHLAWVQTERKSGGLGDLNYPLVSDVTKSISKAFNVLIPDQG
St2-CysPRX 94 IKVKLSEYIGKKYVILFFYPLDFTFVCPTEITAFSDRYEEFEKVNTEVLGVSVDSVFSHLAWVQTERKSGGLGDLNYPLISDVTKSISKSYNVLIPDQG
Ha2-CysPRX 87 IKVKLSDYIGKKYVILFFYPLDFTFVCPTEITAFSDRYAEFEKINTEILGVSVDSVFSHLAWVQTDRKSGGLGDLNYPLVSDVTKSIAKAFNVLIEDQG
Hv2-CysPRX 89 INVKLSDYIGKKYVILFFYPLDFTFVCPTEITAFSDRHEEFEKINTEILGVSVDSVFSHLAWVQTERKSGGLGDLKYPLVSDVTKSISKSFGVLIPDQG
Ta2-CysPRX 85 INVKLSDYIGKKYVILFFYPLDFTFVCPTEITAFSDRHEEFEKINTEILGVSVDSVFSHLAWVQTERKSGGLGDLKYPLVSDVTKSISKSFGVLIPDQG
Zm2-CysPRX 87 INVKLSDYIGKKYVVLFFYPLDFTFVCPTEITAFSDRYEEFEKLNTEVLGVSIDSVFSHLAWVQTDRKSGGLGDLKYPLISDVTKSISKAFGVLIPDQG
At2-CysPRXA 192 IALRGLFIIDKEGVIQHSTINNLGIGRSVDETMRTLQALQYIQENPDEVCPAGWKPGEKSMKPDPKLSKEYFSAI 266
At2-CysPRXB 199 IALRGLFIIDKEGVIQHSTINNLGIGRSVDETMRTLQALQYVQENPDEVCPAGWKPGEKSMKPDPKLSKEYFSAI 273
Cs2-CysPRX 193 IALRGLFIIDKEGVIQHSTINNLGIGRSVDETMRTLQALQYIQENPDEVCPAGWKPGEKSMKPDPKLSKDYFAAI 267
Rs2-CysPRX 189 IALRGLFIIDKEGVIQHSTINNLGIGRSVDETMRTLQALQYIQENPDEVCPAGWKPGEKSMKPDPKLSKEYFSAI 263
Ps2-CysPRX 195 IALRGLFIIDKEGIIQHSTINNLAIGRSVDETMRTLQALQYVQDNPDEVCPAGWKPGEKTMKPDTKLSKEYFSAI 269
Pp2-CysPRX 196 IALRGLFIIDKEGVIQHSTINNLAIGRSVDETKRTLQALQYVQDNPDEVCPAGWKPGEKSMKPDPKLSKEYFSAI 270
Gm2-CysPRX 184 IALRGLFIIDKEGVIQHSTINNLAIGRSVDETKRTLQALQYVQENPDEVCPAGWKPGEKSMKPDPKLSKDYFAAV 258
So2-CysPRX 196 IALRGLFIIDKEGVIQHSTINNLGIGRSVDETLRTLQALQFVQENPDEVCPAGWKPGEKSMKPDPKLSKEYFAA- 269
St2-CysPRX 193 IALRGLFIIDKEGVIQHSTINNLGIGRSVDETLRTLQALQYVQENPDEVCPAGWKPGEKSMKPDPKGSKEYFASI 267
Ha2-CysPRX 186 IALRGLFIIDKEGVIQHSTINNLAIGRSVDETMRTLQALQYVQENPDEVCPAGWKPGEKSMKPDPKLSKEYFAAV 260
Hv2-CysPRX 188 IALRGLFIIDKEGVIQHSTINNLGIGRSVDETLRTLQALQYVQENPDEVCPAGWKPGEKSMKPDPKGSKEYFAAI 262
Ta2-CysPRX 184 IALRGLFIIDKEGVIQHSTINNLGIGRSVDETLRTLQALQYVQENPDEVCPAGWKPGEKSMKPDPKGSKEYFAAI 258
Zm2-CysPRX 186 IALRGLFIIDKEGVIQHSTINNLAIGRSVDETMRTLQALQYVQENPDEVCPAGWKPGERSMKPDPKGSKEYFAAV 260

Figure S4: **Sequence alignment of plant 2-Cys peroxiredoxins.**

NCBI or Genbank references: *Arabidopsis thaliana* 2-Cys PRXs A and B, NP_187769.1 and NP_568166.1, respectively; *Camelina sativa* (Cs), XP_010464879.1; *Raphanus sativus* (Rs), XP_018493095.1; *Papaver somniferum* (Ps), XP_026426631.1; *Prunus persica* (Pp), XP_007202444.1; *Glycine max* (Gm), NP_001341836.1; *Spinacia oleracea* (St), XP_021867340.1; *Solanum tuberosum* (St): XP_006339159.1; *Helianthus annuus* (Ha), XP_021984163.1; *Hordeum vulgare* (Hv), BAJ98505.1; *Triticum aestivum* (Ta), SPT18356.1; *Zea mays* (Zm), NP_001137046.1. The motifs A and B, involved in hyperoxidation resistance of 2-Cys peroxiredoxins (Bolduc *et al.*, 2018), are highlighted in blue and yellow, respectively. The GGLG and YF motifs considered as a signature of sensitivity to hyperoxidation are highlighted in gray. The two catalytic Cys are highlighted in purple. Black bars indicate sequence divergence within motifs A and B.